Phytosterols in human serum as measured using a liquid chromatography tandem mass spectrometry

Yu Chun Teng[1], Marie Claire Gielen[1], Nina M De Gruijter[2], Coziana Ciurtin[2,3], Elizabeth C. Rosser[2,3], Kersti Karu[1]

[1]UCL Chemistry Mass Spectrometry Facility, 20 Gordon Street, University of London, London WC1H 0AJ, UK. [2]Center for Adolescent Rheumatology Versus Arthritis at University College London, University College London and Great Ormond Street Hospitals, London, UK, [3]Center for Rheumatology Research, Division of Medicine, University College London, UK

ABSTRACT

Phytosterols are lipophilic compounds found in plants with structural similarity to mammalian cholesterol. They cannot be endogenously produced by mammals and therefore always originate from diet. There has been increased interest in dietary phytosterols over the last few decades due to their association with a variety of beneficial health effects including low-density lipoprotein cholesterol lowering, anti-inflammatory and anti-cancerous effects. They are proposed as potential moderators for diseases associated with the central nervous system where cholesterol homeostasis is found to be imperative (multiple sclerosis, dementia, etc.) due to their ability to reach the brain. Here we utilised an enzyme-assisted derivatization for sterol analysis (EADSA) in combination with a liquid chromatography tandem mass spectrometry (LC-MS^n) to characterise phytosterol content in human serum. As little as 100 fg of plant sterol was injected on a reversed phase LC column. The method allows semi-quantitative measurements of phytosterols and their derivatives simultaneously with measurement of cholesterol metabolites. The identification of phytosterols in human serum was based on comparison of their LC retention times and MS^2, MS^3 spectra with a library of authentic standards. Campesterol was found at 12.00±2.68 ng/mL, β-sitosterol at 8.50±2.65 ng/mL and fucosterol was at lowest concentration at 1.50±0.84 ng/mL (n=6, healthy individuals). This analytical methodology could be applied to the analysis of other biological fluids and tissues.

1. Introduction

Plant sterols and plant stanols also referred as phytosterols, are a class of lipophilic compounds found in plants with high structural similarity to cholesterol, a well-known molecule endogenously found in humans, particularly notorious for its relation to cardiovascular disease (CVD) [1-3]. Phytosterols are components of plant membranes, which, like cholesterol, regulate membrane fluidity and permeability [4]. Since phytosterols cannot be endogenously produced by mammals they originate from dietary uptake, food such as in vegetables, fruits, grains, cereals, vegetable oils and margarines [2, 5, 6]. Phytostanols are mainly ingested through cereal and cereal derived products (bread), rye and wheat [7]. Cholesterol on the other hand, can be endogenously produced by both animals and plants. More than 250 steroids have been described in plants [7-9]. The most frequently occurring plant sterols are β-sitosterols, sitostanol, campesterol and stigmasterol in food and human body [10, 11]. Plants also contain cholesterol both free and esterified. Cholesterol averages around 50 mg/kg of total lipid in plants, whereas in mammals it can be as high as 5 g/kg (or more) [12]. The Food and Drug Administration (FDA) and the European Food Safety Authority (EFSA) recognize phytosterols as *"safe"* and have authorized health claims regarding risk reduction of coronary heart disease with a daily dietary intake of at least 2 g/day [13, 14]. This has led to increased availability and consumption of phytosterol fortified foods and food supplements. During the digestive process, phytosterols and phytostanols are absorbed in the jejunum through a mechanism like cholesterol absorption [2, 15]. The daily intake in a typical western diet averages to about 300 mg for phytosterols and 20 mg for phytostanols [16-18]. However, their absorption efficacies are reported to be much lower; >2% and >0.02% for phytosterols and phytostanols respectively. In contrast, the absorption efficiency for cholesterol is estimated at 50-60% [3, 19, 20]. This can be explained by the mechanism through which sterols is absorbed. Cholesterol is incorporated in mixed micelles in the intestine which act as carriers for delivery to enterocytes where esterification by acetyl coenzyme A/cholesterol acetyl transferase 2 (ACAT2) occurs, following enterocytes incorporation them into chylomicrons for delivery to the liver. ACAT2's specificity for cholesterol consequently results in relatively less esterification of phytosterols due to steric hinderance leading to reduced absorption [2, 20, 21]. Once delivered to the liver, they are readily excreted by hepatocytes [20]. Only a fraction of ingested phytosterols end up in the lipid carriers of blood resulting in significantly lower levels found in serum compared to cholesterol [19-21].

Sterols are chemically composed of a steroid core including a hydrated phenanthrene (A, B and C ring) fused with a cyclopentane (D ring), a hydroxyl group on C3 of the A-ring, a methyl

groups attached at C18 and C19, and variable C17-side chain (R) attached to the D-ring (Figure 1a,b). The difference between distinct sterols lies in the addition of an extra methyl, ethyl or hydroxyl group to the side chain or/and the steroid core. R groups of phytosterols typically contain nine or ten carbons, as opposed to eight in cholesterol [4]. In contrast to plant sterols, plant stanols contain a saturated core. (Figure 1d). Phytosterols can occur free forms and in four conjugated forms in which the hydroxyl group at C3 is esterified with a fatty acid (FA) or hydroxycinnamic acid (HA) and glycosylated to a hexose (GH) or acyl hexose (AGH) (Figure 1c). Phytosterols and cholesterol can be oxidized to oxyphytosterols and oxysterols respectively (Figure 1d). Oxyphytosterols are present in low levels in food but are tentatively endogenously produced in humans following intestinal absorption by similar biochemical pathways as oxysterols [4, 14, 22]. Both cholesterol and phytosterols are prone to be autoxidized under conditions such as heat and light during food processing, or by reactive oxygen species in tissues [23, 24]. Sterols can be oxidized by endogenous enzymes. Oxyphytosterols in food such as 7-oxo, 7-hydroxy-, and 5,6-epoxy-phystosterols are autoxidized on the sterol-ring (Figure 1d), while side-chain oxidation is mediated by specific enzymes [3, 14]. For example, 24-hydroxycholesterol and 27-hydroxycholesterol are hydroxylated by cytochrome P450 oxidase CYP46A1 and CYP27A1, respectively. Plat J reported an average serum cholesterol concentration in the general population around 5 mmol/L, whereas concentrations of plant sterols by 400 times lower and stanols by 100,000 times lower than cholesterol [14].

Over 20% of free cholesterol in humans is found in the brain where steady cholesterol homeostasis is essential for proper functioning of neurons [25]. Cholesterol biosynthesis and metabolism is tightly regulated in the central nervous system (CNS) [26, 27]. Cholesterol homeostasis is essential for proper brain functioning and dysregulation of cholesterol metabolism can lead to neurological problems. Pathophysiological studies have linked disturbed metabolism of cholesterol to neurological and neurodegenerative diseases such as multiple sclerosis, Alzheimer's disease and dementia [1, 2, 10, 14]. Phytosterols have been proposed to have therapeutic effects in the pathogenesis of neurodegenerative diseases, potentially by modulating cholesterol homeostasis in CNS [21, 28]. As phytosterols have been supplemented in functional food products, this leads to increase dietary exposure of both phytosterols and oxidation products [3, 12, 29]. Recent studies show that phytosterols can cross the blood brain barrier (BBB) and accumulate in the membranes of CNS cells [3, 10]. Based on this finding, researchers have started to investigate the physiological role of phytosterols and their oxidation products are constantly researched [3]. One study showed that increased dietary intake of

phytosterols significantly reduced the onset and severity of experimental autoimmune encephalomyelitis in SJL mice, the most accepted animal model for the study of Multiple Sclerosis [10]. In addition, phytosterols are suggested to have anti-inflammatory and anti-cancerous properties [7, 8, 24]. Exact molecular mechanisms regarding the modes of action of phytosterols are still lacking and further elucidation is required [13, 21]. Furthermore, potential detrimental health effects have been suggested as well [29]. Increased phytosterol intake has shown decreased bioavailability of β-carotene (vitamin A precursor) and α-tocopherol (vitamin E) [12].

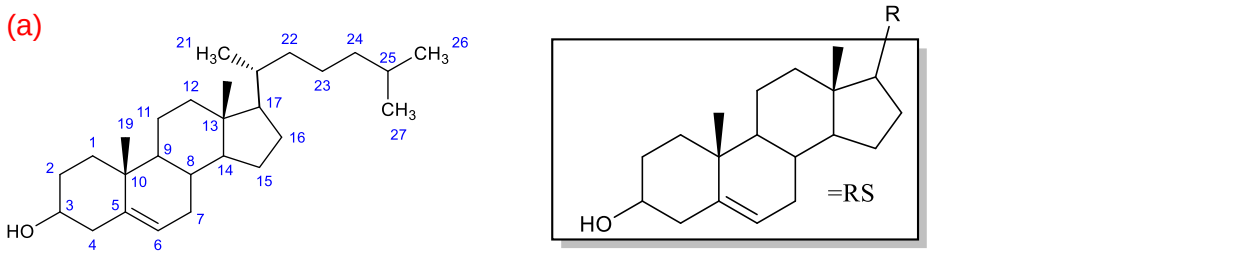

Cholesterol
R= rest group

Plant sterols, RS = rest steroid group,

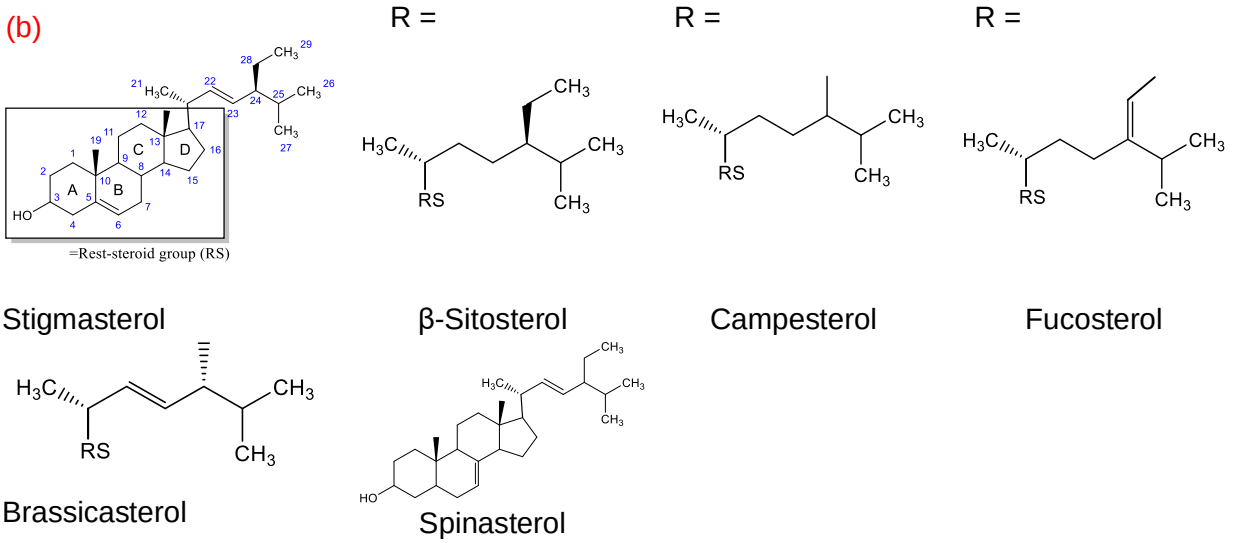

Stigmasterol

β-Sitosterol

Campesterol

Fucosterol

Brassicasterol

Spinasterol

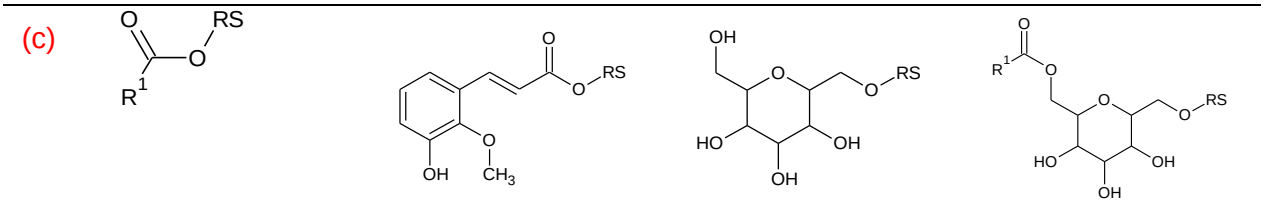

Fatty acid (FA)

Hydroxycinnamic acid (HA)

Hexose (GH)

Acyl-hexose (AGH)

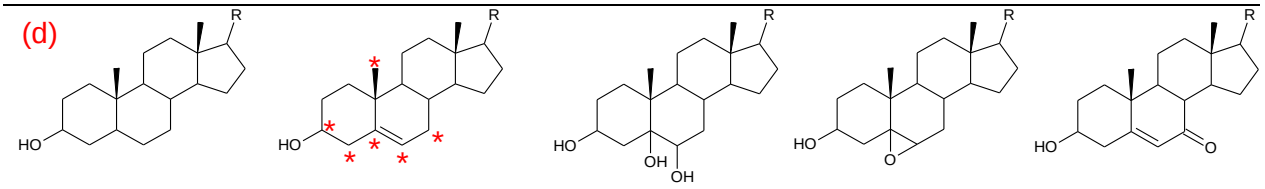

Stanols

Oxysterols

Diols plant sterols

Epoxy plant sterol

7-oxo plant sterols

Figure 1. Chemical structures of plant sterols and their derivatives. Most phytosterols (PS) have the same rest-steroid (A, B, C, D rings) core (RS). (A) Basic structure of sterol with respective

numbering. The rest group (R) is a carbon chain. (B) The most abundant phytosterols:- campesterol, β-sitosterol, brasicasterol, fucosterol, stigmasterol and spinasterol. (C) The four main conjugates of PS. The hydroxyl group at C3 is esterified to a fatty acid (FA), where R1 is the carbon chain of the fatty acid or hydroxycinnamic acid (HA) or glycosylates to a hexose (HA) or acyl-hexose (AGH). The C3 hydroxyl group of HA is esterified to ferulic acid (here shown) or p-coumaric acid and AGH has a fatty acid that is esterified to the 6-OH of the hexose moiety. (D) Plant stanols, which contain a saturated core, also possible oxidation points on (plant) sterols are shown by asterisk and examples of diols, epoxy, and 7-oxo (plant) sterols.

Many methodologies were exploited to analyze phytosterols in biological samples, from the traditional methods using thin-layer chromatography (TLC), to liquid chromatography (LC) [11, 13, 30, 31]. Nowadays, phytosterols and their oxidation products analyzes are dominated by GC-MS using selected-ion monitoring (SIM) mode or LC-MS/MS method combined with multiple reaction monitoring (MRM) mode [32, 33]. In summary, the protocol usually starts with the addition of ethylenediaminetetraacetic acid (EDTA) and butylated hydroxytoluene (BHT) to preserve the blood samples, following by alkaline hydrolysis to unesterified lipids. For only measuring free sterols (non-esterified), hydrolysis is omitted. After hydrolysis, solid-phase extraction is the most common technique to extract sterols from blood samples. Classically for GC-MS analysis, sterols are derivatized to their trimethylsilyl ester (TMS) derivatives to enhance sensitivity and volatilization prior to GC-MS analysis [30, 34, 35]. Thermal decomposition to biological samples was inevitable during the vaporization in GC, also derivatization groups possibly eliminate in the ion source, which makes it difficult to determine the molecular weight of unknown sterols [31, 36]. The LC-MS/MS analyzes are current popular choice [37]. To enhance sensitivity of measurements and phytosterol solubility, different derivatization agents were used to transform sterols to their picolinyl ester-, [38] nicotinyl esters-, [39] and Girard P (GP) hydrazones [30, 40, 41]. Here, we report utilization of an enzyme-assisted derivatization for sterol analysis (EADSA) technology for the detection of phytosterols in human serum. EADSA is a chemical approach, which consists of enzymatic conversion of a 3β-hydroxy-5-ene group or a 3β-hydroxy-5α-hydrogen-containing stereochemistry of sterols to 3-oxo-4-ene and 3-oxo sterols followed by tagging a positively charged quaternary nitrogen group to the resulting oxo group in a “click reaction” (Figure 2). In summary, the 3β-hydroxyl groups (OH, molecular weight = 17.01 Da) of sterols are turned into permanent positive charge-tagged GP moiety ($C_7H_8N_3O^+$, molecular weight = 150.16 Da) and this increases the mass of sterol by 132.14 Da. The advantage of EASDA is it increases the solubility of these molecules during LC-MS analysis and also enhances signal under ESI condition by 1,000, in comparison to underivatized sterols versions [42, 43]. Most importantly, sterol GP-hydrazones generate informative MS^3 ($[M]^+ \rightarrow [M-$

79]$^{+}$→) spectra benefiting their structural elucidation [44, 45]. After GP-derivatization, we purified O/GP sterols and removed an excess of GP-reagent using a SPE C_{18} cartridge. We analyzed the resulting samples using a capillary LC coupled to a linear ion trap mass spectrometer.

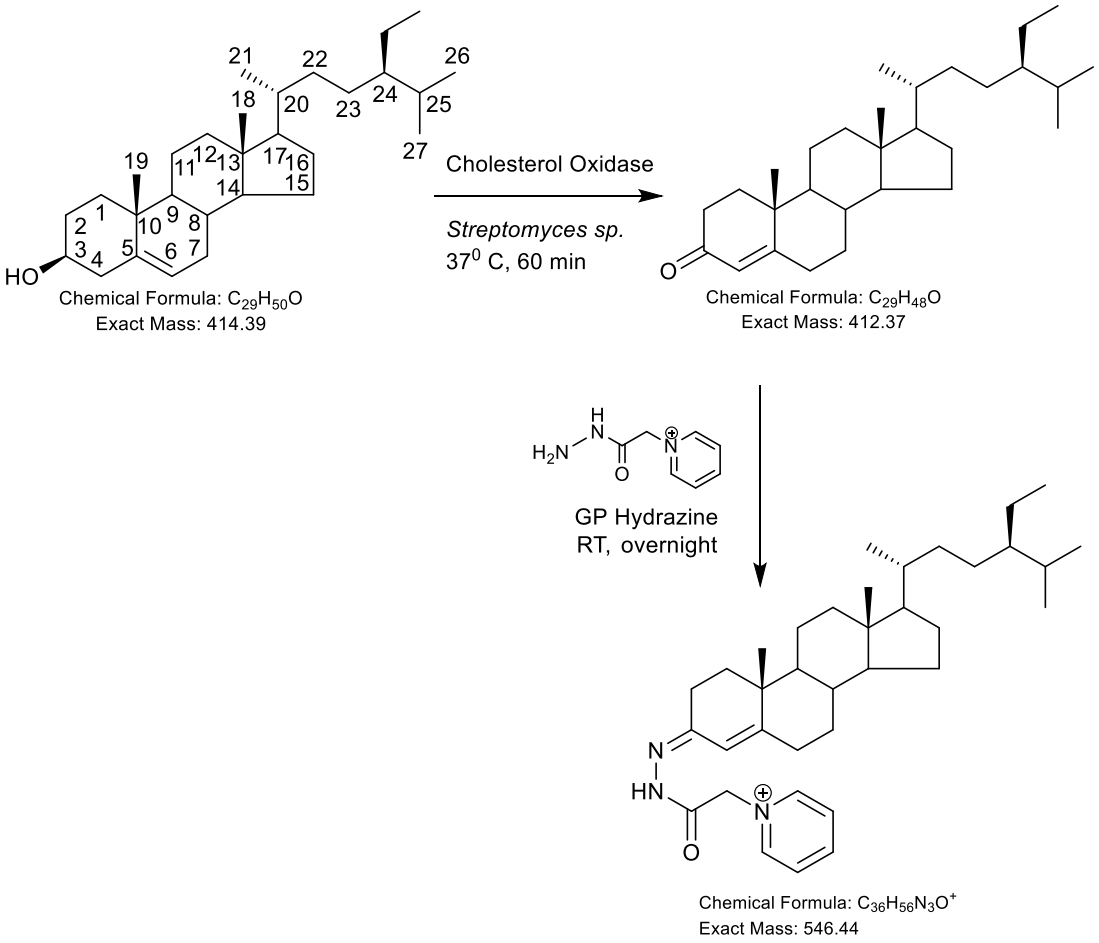

Figure 2. Enzyme-assisted derivatization for sterol analysis EASDA. Example is shown for β-sitosterol, of which 3β-hydroxy group was converted to 3-oxo group followed by GP reagent derivatization to GP hydrazone, O/GP β-sitosterol.

2. Materials and methods

2.1. General

High-performance liquid chromatography (HPLC)-grade water, absolute ethanol, and other HPLC-grade solvents were from Fisher Scientific (Loughborough, UK) or Sigma-Aldrich (Dorset, UK). Acetic acid was AnalaR NORMAPUR grade (BDH, VWR, Lutterworth, UK). Cholesterol (5-cholesten-3β-ol), cholestanol (5α-cholestan-3β-ol), lathosterol (7,5α-cholesten-3β-ol),

desmosterol (5,24-cholestadien-3β-ol), fucosterol (5-cholesten-24(28)-ethylidene-3β-ol), campesterol (5-cholesten-24-methyl-3β-ol), β-sitosterol (5-cholesten-24β-ethyl-3β-ol), stigmasterol (5,22-cholestadien-24β-ethyl-3β-ol), brassicasterol (5, 22-cholestadien-24β-methyl-3β-ol), 7-keto-β-sitosterol (5-cholesten-24-ethyl-3-ol-7-one), were purchased from Steraloids, Inc. (Newport, R.I., USA). [25, 26,26,26,27,27,27,27-$^{2}H_{7}$] Cholesterol [$^{2}H_{7}$]-Cholesterol was purchased from Avanti Polar Lipids (Alabama, USA). All reference sterols were stored at -20°C. Desmosterol was wrapped in foil because of its sensitivity to light. Cholesterol oxidase from *Streptomyces sp.* was from Sigma-Aldrich (Dorset, UK). Girard P (GP) reagent (1-(carboxymethyl)pyridinium chloride hydrazide) was from Santa Cruz Biotechnology, Inc. Certified Sep-Pak C_{18} SPE cartridges (3 cc, 200 mg) were from Waters (Elstree, UK). Luer-lock syringes were from BD Biosciences (Sigma-Aldrich). Glacial acetic acid (99.9%) was from Sigma-Aldrich (Dorset, UK). Formic acid (LC-MS grade) was from Fisher Scientific, Inc. (Loughborough, UK). HPLC grade chloroform, dichloromethane, propan-2-ol and ethanol and LC-MS grade methanol, water and acetonitrile were from Honeywell, Fisher Scientific and/or VWR. Potassium phosphate monobasic (KH_2PO_4, ≥99.5%) was from Honeywell (Seelze, Germany). All necessary plastic materials used were as described in Griffiths, etc [46].

2.2. Human samples

The blood samples were collected from six healthy volunteers of age 23 to 30, three females and three male, with BMI 18 to 22 during public engagement events (including young scientist days) organized by the Center for Adolescent Rheumatology Versus Arthritis, Division of Medicine, University College London (UCL). Two blood samples were collected from patients with Juvenile Onset Systemic Lupus Erythematosus (JSLE) attended the adolescent and young adult lupus clinics at University College London Hospital, females ages 20 and 26 with BMI 20. Two samples were from patients with alternating hemiplegia of childhood (AHC), female and male age 33, BMI 22. Informed written consent or parental consent/participant assent was acquired from both patients and healthy volunteers as age-appropriate under the ethical approval reference: REC11/LO/0330 and in accordance with the Declaration of Helsinki. All information was stored as pseudo-anonymised data. Blood serum was used for mass spectrometry analyses. The blood serum samples were collected in serum gel S/9 monovette® (Sarstedt). Serum was separated from blood cells by centrifugation at 3500 rpm for 10 min at 18 °C (Heraues multifuge 4KR centrifuge, Osterode, Germany). To avoid autoxidation 10 µL of a methanolic butylated hydroxytoluene (BHT 25 mg/ml) solution was added to 1 mL serum.

2.3. Enzyme-assisted derivatization (EADSA)

Authentic standards of phytosterols were dissolved in ethanol to make 1 µg/µL stock solutions. Next, 2 µL of stock solution was added into 98 µL of propan-2-ol in a 5 mL round-bottom flask followed by addition of phosphate buffer solution (1 mL, 50 mM KH_2PO_4, pH 7) containing 3 µL cholesterol oxidase from *Streptomyces sp.* (2 $mgmL^{-1}$, 44 $units{\cdot}mg^{-1}$). The mixture was incubated at 37 °C for 60 min to convert 3β-hydroxy-5-ene moiety to 3-oxo-4-ene. The oxidation was quenched with 2 mL methanol. Glacial acetic acid (150 µL) and GP hydrazine (150 mg) were added. The mixture was left overnight to derivatise 3-oxo-4-ene sterols to GP hydrazones.

2.4. Recycling solid phase extraction

Recycling SPE was carried out to remove excess GP reagent as previously published [23, 46]. A 200 mg Sep-Pak Vac cartridge was washed with 6 mL 100% methanol, followed by 6 mL 10% methanol, and then conditioned with 4 mL 70% methanol. Consequently, the reaction mixture (3.25 mL), was loaded onto the C18 cartridge, followed by 1 mL 70% methanol (used to rinse the reaction tube). The eluent was diluted with 4 mL water to 35% methanol. The combined effluent (5 mL) was collected into the glass beaker and diluted with water (4 mL) to give 9 mL of 35% methanol. The resulting solution was re-applied to the C18 cartridge, and the effluent was collected and further diluted with 9 mL water to give a 18 mL of 17.5% methanol. The cartridge then was washed with 1 mL of 17.5% methanol and the wash was then combined to give a resultant solution of 19 mL 17.5% methanol. Next, the resulting solution was applied again on the C18 cartridge, and the effluent was discarded. At this point, most GP-hydrazones were retained on the C18 cartridge. The cartridge was then washed with 6 mL 10% methanol. Our validation experiments confirm required volumes of elution solvents required to elute fully derivatized phytosterols (Appendix A). We found that cholesterol- and phytosterol-GP-hydrazones eluted with three 1-mL portions of 100% methanol and collected in 1.5 mL-microcentrifuge tubes (SPE-2-Fr1, 2, 3), followed by four 1-mL portions of 100% ethanol (SPE-2-Fr-4, 5, 6, 7) and another application of two 1-mL portions of 100% DCM (SPE-2-Fr-8, 9) from the SPE-2 C_{18} cartridge.

2.5. Extraction of phytosterols from human serum

One hundred mL of serum was added drop-wisely into a 2-mL Eppendorf tube containing 1 mL of absolute ethanol and 0.5 µL of [$^2H_7$] cholesterol (1 µg/µL in propan-2-ol). The sample was sonicated for 5 min. Then, 330 µL of water was added to the tube and ultrasonicated for a further 5 min, and the sample was then centrifuged at 14,000 *x*g at 4°C for 30 min. The resulting sample contained 70% ethanol. A 200-mg Sep-Pak C_{18} cartridge was rinsed with 4 mL of ethanol and then conditioned with 6 mL of 70% ethanol. We adapted a previously published protocol [44] where authors validated the method with a solution of cholesterol and 24(R/S)-

[26,26,26,27,27,27-$^{2}H_6$] hydroxycholesterol in 70% ethanol, they found that cholesterol was retained on the column even after a 5.5-mL column wash of 70% ethanol, whereas 24(R/S)-[26,26,26,27,27,27-$^{2}H_6$] hydroxycholesterol elutes in the flow-through and column wash. They also mentioned that after a further column wash with 4 mL of 70% ethanol, cholesterol was eluted from the column in 2 mL of absolute ethanol. They further applied an additional 2 ml of absolute ethanol on the column to elute more hydrophobic sterols. Therefore, in this work, the flow-through (1.43 mL) and a column wash of 9.5 mL of 70% ethanol were collected in a 15 mL round-bottom flask to elute more polar phytosterols from the column (Figure S1). As some phytosterols are more lipophilic than cholesterol, therefore we eluted them in 8 mL ethanol (Figure S1, fraction B). Just mention here we applied sequentially 1 mL of ethanol eight times on the cartridge. The cartridge was further stripped with 2 mL DCM to elute even more lipophilic phytosterols (Figure S1, fraction C). All three fractions were combined into the same round-bottom flask. Finally, the solvent was dried using a rotary evaporator. Then the samples were reconstituted with 100 µL propan-2-ol and thoroughly vortexed, before they were subjected to cholesterol oxidation, GP-derivatization and SPE-2 on a C18 column, as described above.

2.6. Direct infusion single-stage TOF-MS

A Premier XE TOF-MS connected to a 2777C autosampler was utilized to screen SPE2 fractions for each sample. The ESI was operated in positive mode. The capillary voltage was 2.5 kV and sample cone voltage was 50 V. The desolvation and source temperatures were 150 °C. The desolvation gas flow was 450 L/h and the cone gas flow was 100 L/h. The mass range was *m/z* 100-800 and the scan rate was 1 s^{-1}. Samples (10 µL) were directly infused in 50% of mobile phase A (MeOH, Propan-2-ol, Formic acid 50:50:0.1, *v/v/v*) and 50% mobile phase B (MeOH, Formic acid 100:0.1, *v/v/v*) with a flow of 0.2 mL/min. The analysis time was 2 minutes. Then, one fraction for each the O/GP derivatized phytosterol with the highest $[M]^+$ signal was selected for a LC-MS^n analysis.

2.7. Direct infusion ES multi-stage fragmentation mass spectrometry

A Thermo Finnigan LTQ linear ion trap mass spectrometer (Thermo Fisher Scientific, UK) was operated with the following settings: - spray voltage 1.00 to 1.20 kV, capillary temperature 200^0C, no sheath or auxiliary gas used. The mass range *m/z* 50 – 700 was scanned, and centroid data was collected. MS, MS^2 and MS^3 spectra were recorded. MS^2 experiment was performed on a precursor ion. MS^2 spectra were dominated by $[M-79]^+$ and $[M-107]^+$ fragment ions. MS^3 scans were performed on fragment-ions resulting from a neutral loss of 79 Da or 107 Da in the MS^2. For acquisition of both MS^2 and MS^3 spectra, the collision energy setting was

35% with the isolation width at 1.00. MS, MS^2 and MS^3 scans consisted of three averaged micro scans each with a maximum injection time of 200 ms.

2.8. Capillary-LC-ES-MS^n

LC-MS^n analyzes were performed using an Accela HPLC system interfaced to the LTQ MS. The LC system is comprised of an autosampler, degasser and pump system. The injection volume was 10 µL. Chromatographic separation was achieved on a Hypersil Gold C_{18} column (1.9 µm particles, 100 mm x 21 mm, Fisher Scientific). Mobile phase A was composed of 33.3% methanol, 16.7% acetonitrile, with 0.1% formic acid and mobile phase B was 60% methanol, 40% acetonitrile, 0.1% formic acid. Initially B was at 50% and was raised to 70% over 3 min, then was raised to 99% B over the next 17 min and stayed at 99% B for 3 min, before returning to 50% B in 6 s and re-equilibrating for a further 5 min 54 s, giving a total analysis time 26 min. The flow rate was 180 µL/min. The eluent was directed to the ESI source of the LTQ mass spectrometer. The ESI was operated in positive mode with a capillary temperature of 280 °C. The spray and capillary voltages were set to 4.5 kV and 33 V respectively. The sheath, auxiliary and sweep gas flow rates were 40, 10 and 0 respectively. The ion trap analyzer set-up for seven scan events during one LC-MS analysis. In event 1 full scan of *m/z* 80-600, then follows by other 6 events set either for MS^2 and/or MS^3 scans. MS^2 transition was set on an expected derivatized phytosterols or predicted their metabolites/autoxidation products. The MS^3 scans were performed on fragment-ions resulting from a neutral loss of 79 Da and 107 Da in the MS^2, $[M]^+ \rightarrow [M\text{-}79]^+ \rightarrow$, and $[M]^+ \rightarrow [M\text{-}107]^+ \rightarrow$. A precursor-ion include list for and MS^3 $[M]^+ \rightarrow [M\text{-}79]^+ \rightarrow$, transitions for potential oxyphytosterols were set-up. MS^1, MS^2 and MS^3 scans contain three averaged microscans, each with a maximum ion fill time of 200 ms. For MS^2 and MS^3 the isolation width was set to 1 *m/z* for the selection of precursor-ions and the normalized collision energy was 35%. For the analysis of GP-tagged phytosterols from serum, 46.65 µL of the combined SPE-2 fractions (7mL) from the second Sep-Pak C_{18} cartridge (SPE-2-Fr1 to 7) was diluted with 28.36 µL of ACN, 25 µL 0.1% FA in water. Each SPE-2 fraction was also analyzed separately as 46.65 µL of each SPE-2-fraction from each serum sample, was diluted with 28.36 µL of ACN, 25 µL 0.1% FA.

3. Results and discussion

3.1. Mass measurement of authentic standards

Griffiths W. J. *etc* [23, 26, 46-48] developed EADSA technology for sterols analysis which was adapted in this research. Briefly, cholesterol, its precursor desmosterol ($C^{5,24-}$3β-ol), and the plant sterols stigmasterol (24β-ethylcholesta-5,22-dien-3β-ol, $C^{5,22-}$24β-ethyl-3β-ol), sitosterol (24β-ethylcholest-5-en-3β-ol, C^{5}-24β-ethyl-3β-ol), campesterol (24β-methylcholest-5-en-3β-ol, C^{5}-24β-methyl-3β-ol), and brassicasterol (24β-methylcholesta-5,22-dien-3β-ol, $C^{5,22-}$24β-methyl-3β-ol) were oxidized with cholesterol oxidase and derivatized with GP reagent. Cholesterol oxidase converts 3β-hydroxy-5-ene sterols to their 3-oxo-4-ene analogs, and the resulting 3-oxo group derivatized with GP hydrazine giving 3-GP hydrazones. The GP authentic standards were directly infused into the linear ion trap MS, and the MS^1, MS^2 and MS^3 spectra were recorded and established as the reference library. These GP hydrazones give intense $[M]^+$ ion signal upon ESI ionization. For example, O/GP-derivatized β-sitosterol gives a $[M]^+$ ion at *m/z* 546. The MS^2 (546→) spectrum shows $[M-79]^+$ ions at *m/z* 467 and $[M-107]^+$ at *m/z* 439 (Figure 3a). The MS^3 (546→467→) spectrum contains a triad of fragment ions at *m/z* 151, 163, 177 (Figures 3b). A similar triad of fragment ions is observed in the MS^3 ($[M]^+$→$[M-107]^+$→) spectrum, but with the fragment ions displaced in mass by 28 Da, corresponding to additional loss of CO (data not shown). These fragment ions are characteristic of the derivatized 3-oxo-4-ene structure in the absence of additional groups in the A and B rings. They are formed by cleavage in the B-ring and are described by two competing series of b-type fragment ions (Figures 4). The *b ion-series corresponds to B-ring fragment ions which have formed via the $[M-79]^+$ intermediate (which corresponds to the precursor ion having lost the pyridine ring). The *b ion-series of fragment ions are generated in the MS^3 $[M]^+$→$[M-79]^+$→ spectra. These fragment ions are described as *m/z* 151 ($*b_1$-12), 163 ($*b_3$-C_2H_4) and 177 ($*b_2$) (Figure 4) [26, 43, 46-49].

A library of fragmentation patterns MS^2 and MS^3 spectra for sterol GP hydrazones has been established and could be used by researchers for the structure elucidation of GP-tagged sterols [23, 26, 47, 48, 50]. In summary, the *b and $^{\#}$b ion-series are indicative of the sterols possessing a 3-oxo-4-ene group before GP derivatization and a 3β-ol-5-ene structure before treatment with cholesterol oxidase and GP reagent, with no additional substituents in the A and B rings. This pattern changes with the introduction of hydroxy- or oxo-groups in the B rings of sterols.

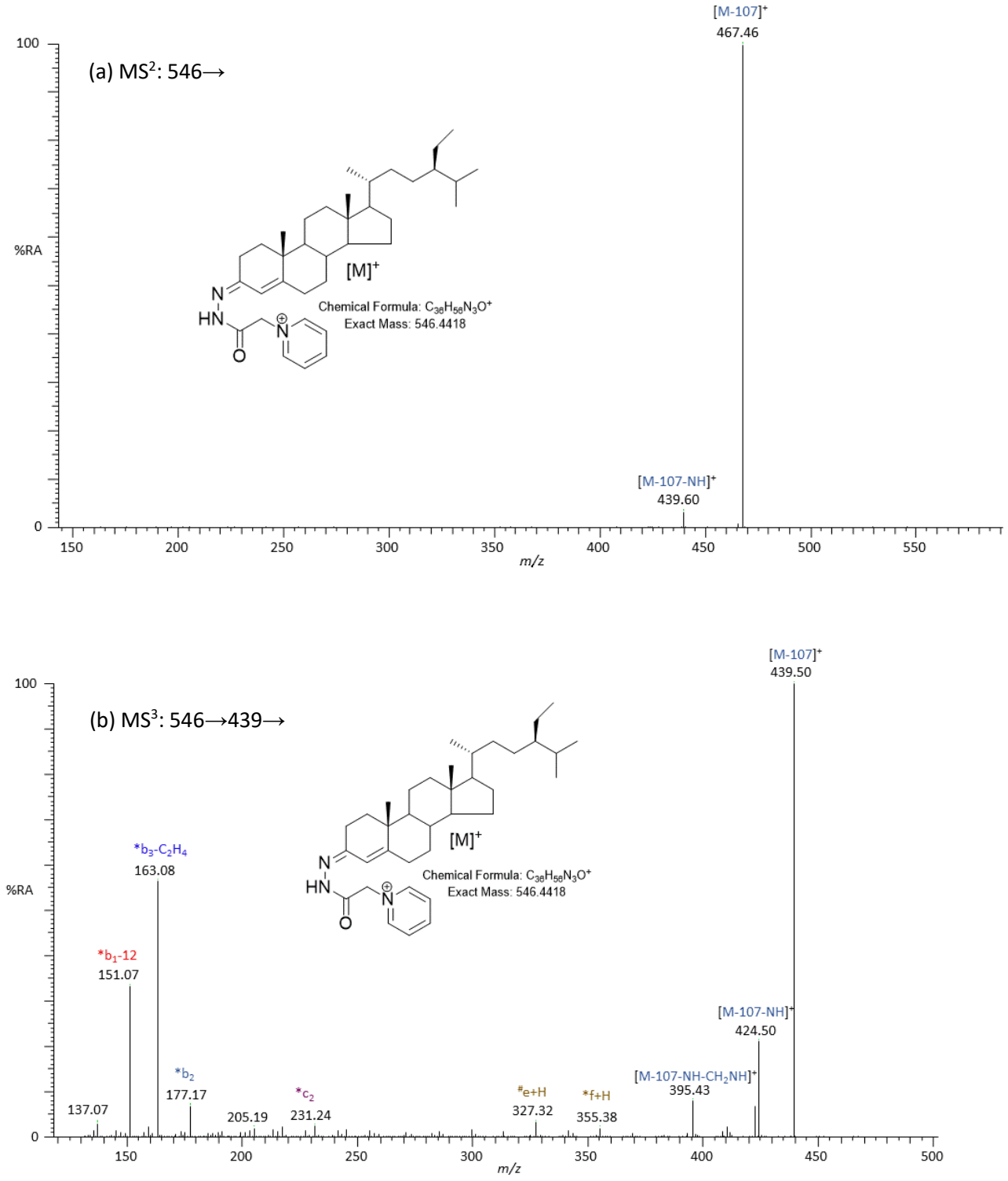

Figure 3. (a) ES-MS^2 (546→); and (b) MS^3 (546→439→) spectra of the oxidized and GP-derivatized β-sitosterol authentic standard.

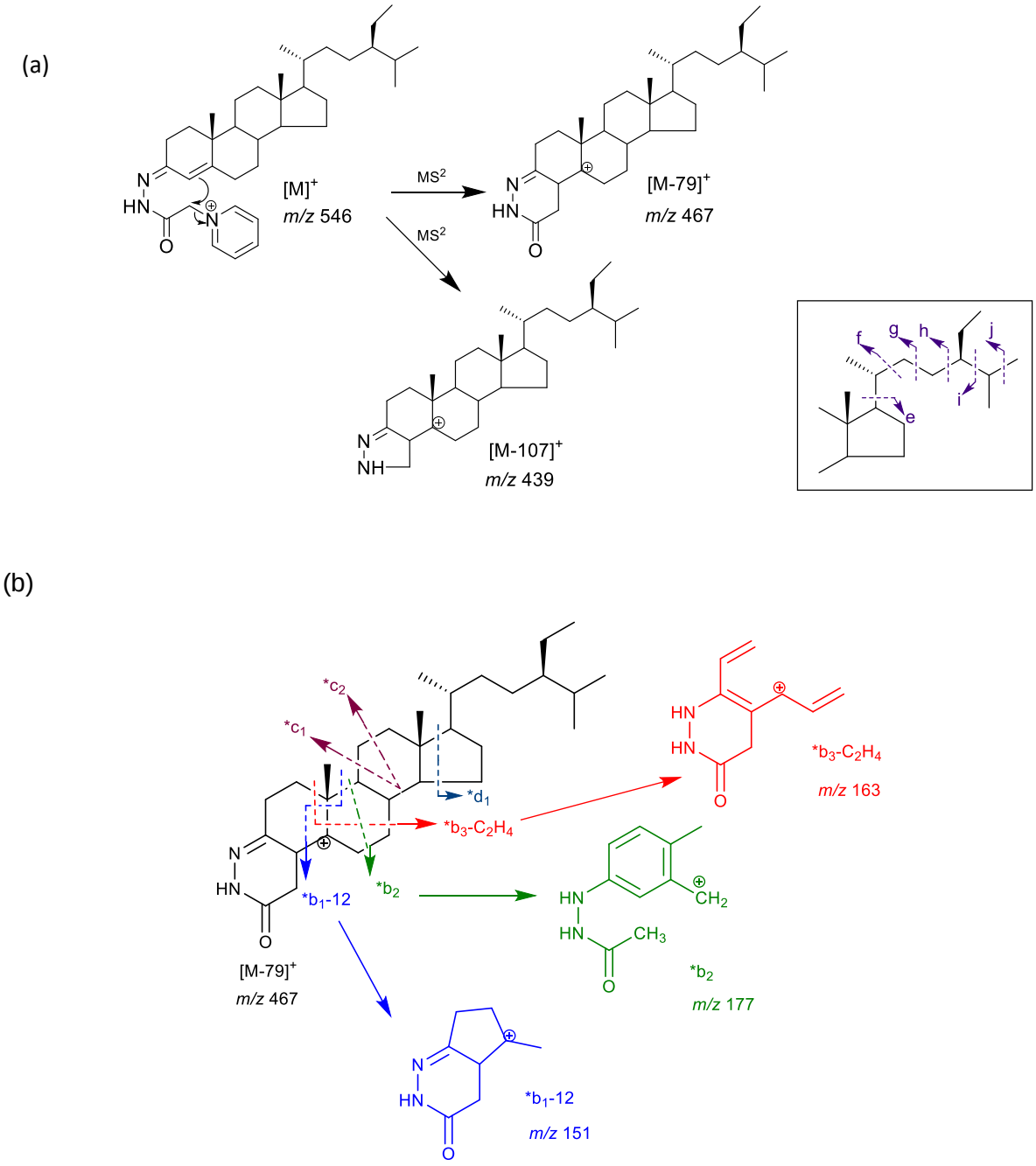

Figure 4. (a) MS^2 fragmentation, (b) MS^3 ($[M]^+ \rightarrow [M\text{-}79]^+ \rightarrow$) fragmentation of the O/GP-derivatized β-sitosterol. An asterisk preceding a fragment-ion describing letter e.g. *b_1-12, indicates that the fragment-ion has lost the pyridine moiety from the derivatising group. A prime to the left of a fragment ion describing letter e.g. '*f, indicates that cleavage proceeds with the transfer of a hydrogen atom from the ion to the neutral fragment. A prime to the right of the fragment describing letter indicates that cleavage proceeds with hydrogen atom transfer to the fragment-ion e.g. *e'. The inset indicates fragmentation in the C-17 side chain of the GP-derivatized sterols. Figures were taken from [23, 43, 46, 49] with permission.

While the major cleavages in the sterol ring system occur in the B-ring and give abundant fragment ions, minor but important fragment ions are generated by cleavages in the C-and D-rings, and in the C-17 side-chain giving the fragment ions of low abundance in MS^3 spectra. In the MS^3 ($[M]^+ \rightarrow [M\text{-}79]^+ \rightarrow$) spectrum for GP-derivatized fragment ions $*c_2$, $*d_1$, $^{\#}$e+H ($^{\#}$e'), and *e+H (*e') are consistently observed at *m/z* 231, 285, 299, 327 for O/GP-derivatized cholesterol, desmosterol, and campesterol (Figures S3-5) [43]. Desmosterol is an intermediate in the *de novo* synthesis of cholesterol. MS^3 ($[M]^+ \rightarrow [M\text{-}79]^+ \rightarrow$) of gives a similar spectrum to those other 3-oxo-4-ene sterols. However, peaks at 353 and 355 corresponding to *f-H ('*f) and *f+H (*f'); and 325 and 327 corresponding to $^{\#}$f-H ('$^{\#}$f) and $^{\#}$f+H ($^{\#}$f'), are of elevated in intensity. These ions are formed by cleavage of the bond between C-20 and C-22.

The MS^3 spectra of the O/GP-derivatized stigmasterol (24β-ethylcholesta-5,22-dien-3β-ol), β-sitosterol (24β-ethylcholest-5-en-3β-ol), campesterol (24β-methylcholest-5-en-3β-ol), and brassicasterol (24β-methylcholesta-5,22-dien-3β-ol) showed the common features of 3-oxo-4-ene sterol GP hydrazones fragmentation of the B-ring. The MS^3 ($[M]^+ \rightarrow [M\text{-}79]^+ \rightarrow$) spectrum of O/GP-β-sitosterol was similar to cholesterol (Figure 3b, Figure S2). However, the peak at 367 in the spectrum of cholesterol (Figure S3c) corresponding to the doubly unsaturated cholestane carbonium ion, shifted to 395, and shifted to 381 in the MS^3 spectrum of the O/GP-derivatized campesterol (Figure S5c). The peak at *m/z* 424 is a loss of C_3H_6 from the side-chain. The MS^3 spectrum of the GP-derivatized stigmasterol is characterised by peaks at 381 (*h+H) both formed because of cleavage of the C-23-C-24 bond (Figure S6). There is also enhanced abundance of fragment ions at *m/z* 284 ($^{\#}$e'-NH), 299 ($^{\#}$e'), and 327 (*e') each formed because of cleavage of the C-17-C-20 bond. The presence of methyl group, rather than an ethyl group, attached to C-24 in brassicasterol leads to the same *e' and *h' fragment ions (Figure S7).

The GP derivatized fucosterol and stigmasterol have the same elemental composition (both *m/z* 544) and were indistinguishable by MS^2 spectra (544→). However, MS^3 (544→465→) of the GP derivatized fucosterol MS^3 spectrum shows the C_{17} side-chain fragment ions at *m/z* 367 (*g-H) and *m/z* 353 (*f-H) with of significant intensities (Figure 5a). Whereas stronger signal of *m/z* 381 (*h+H), *m/z* 327 (*e+H) and *m/z* 284 ($^{\#}$e+H-NH) were observed for the GP derivatized stigmasterol (Figure 5b).

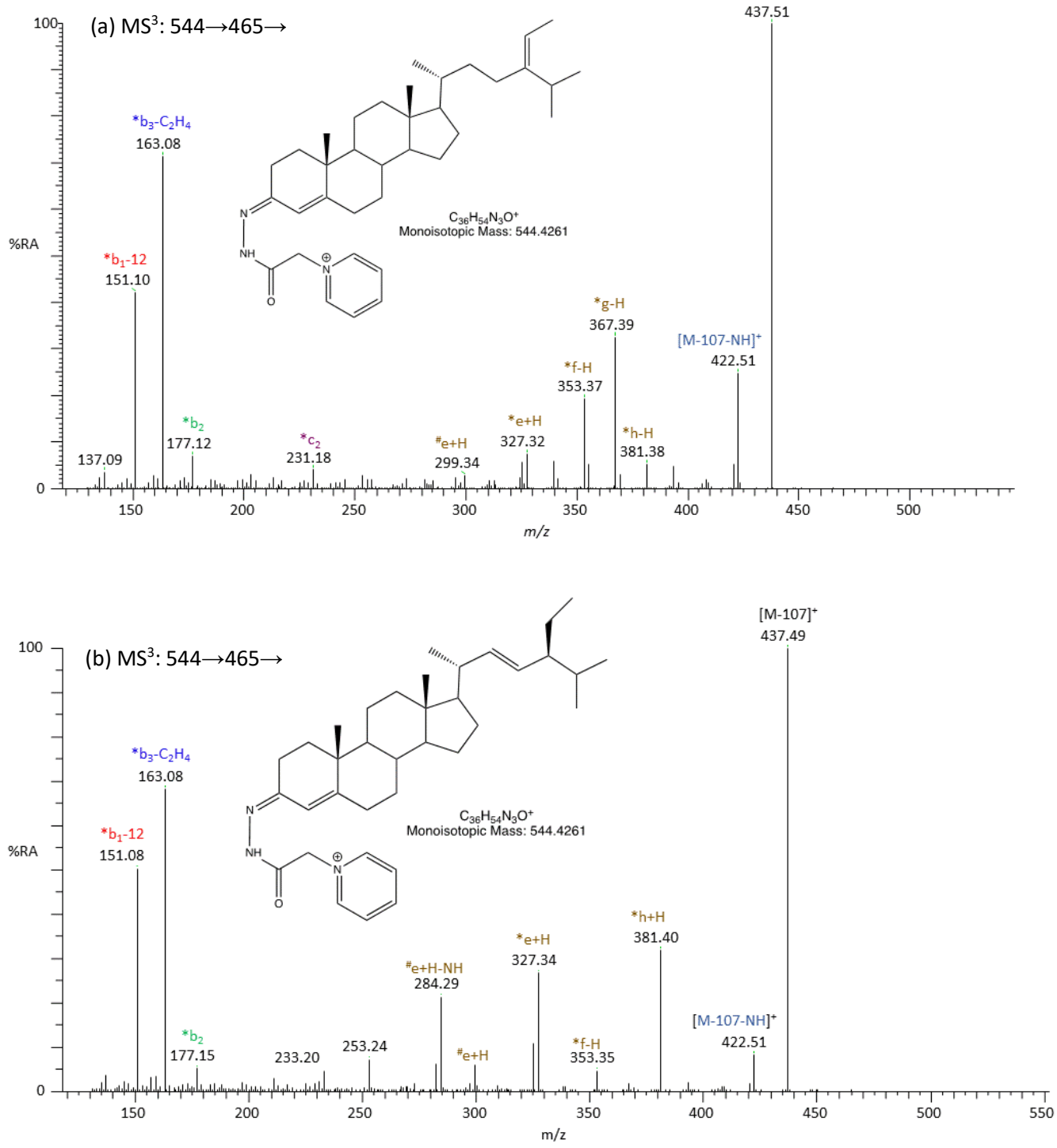

Figure 5. (a) The MS^3 (544→465→) spectra for O/GP fucosterol, (b) O/GP stigmasterol authentic standards.

7-Oxo-β-sitosterol was derivatized by GP hydrazine at C-7 position even though it was oxidized by cholesterol oxidase enzyme during our sample preparation, giving the peak at *m/z* 562 (Supplemental Figure 7a). In contrast to 3-oxo compounds, 7-oxo compounds showed a prominent pattern of fragmentation ions corresponding to $[M\text{-}97\text{-}H_2O]^+$, $[M\text{-}107\text{-}NH]^+$ and $[M\text{-}107]^+$. The MS^3 spectrum (562→483→) of the GP derivatized 7-oxo-β-sitosterol give a minor fragmentation at *m/z* 157/159, which probably consists of the unsaturated diazacyclohexanone ring and remnants of the B-ring.

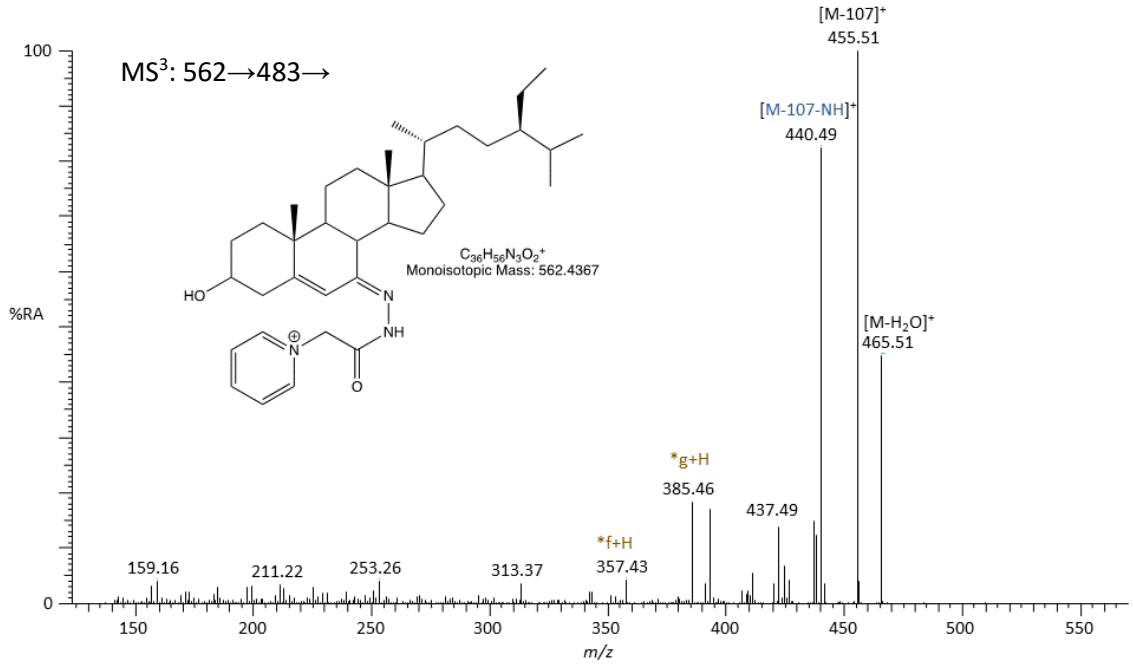

Figure 6. (a) MS^3 (562.5→483.5→) spectrum of O/GP 7-oxo-β-sitosterol authentic standard.

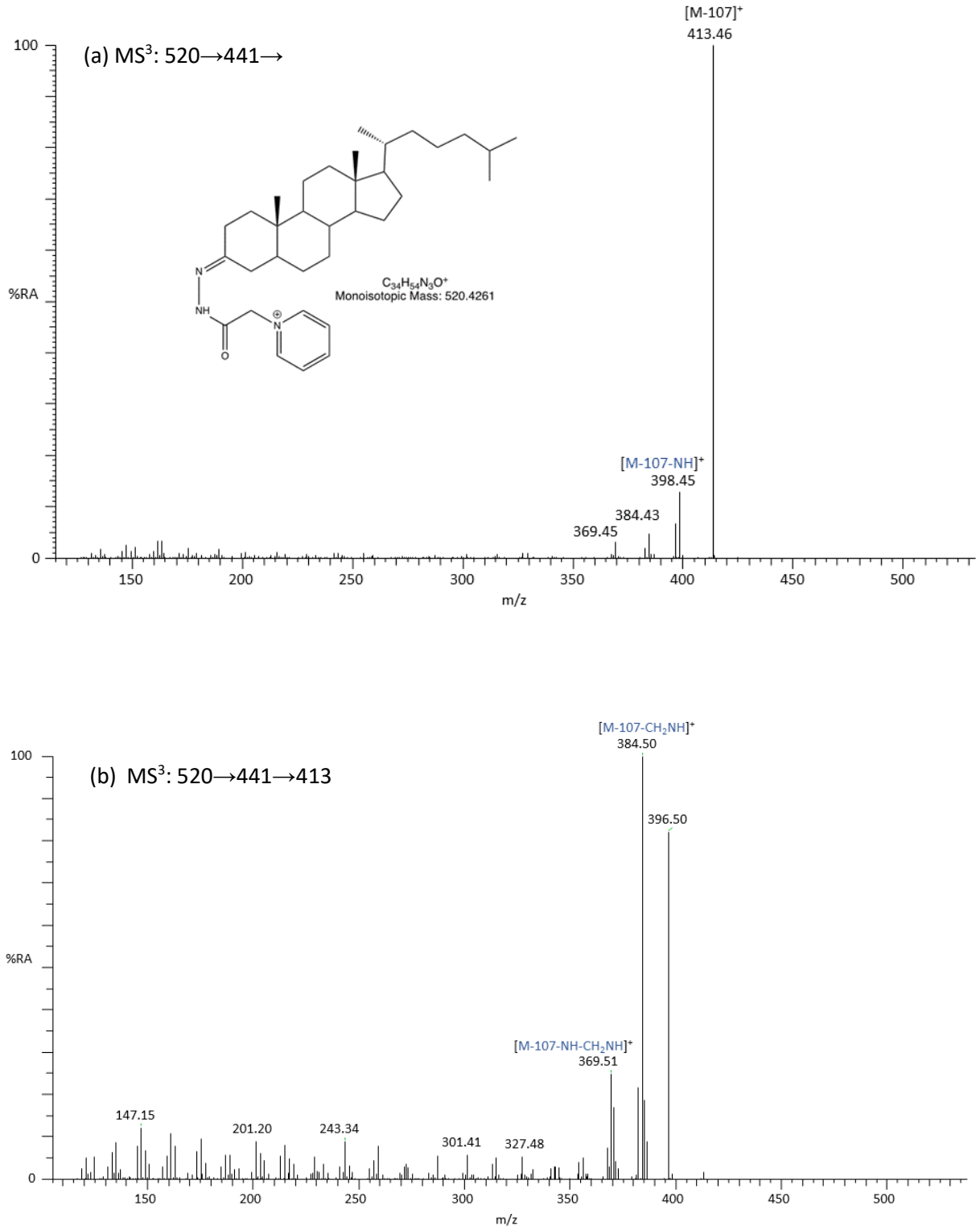

Figure 7. (a) The MS^3 (520.5→441.5→) spectrum, and (b) MS^4 (520.5→441.5→413.5→) spectrum of O/GP-derivatized cholestanol authentic standard.

MS^3 ($[M]^+ \rightarrow [M\text{-}79]^+ \rightarrow$) spectra, both O/GP-derivatized cholestanol and lathosterol showed a strong signal at *m/z* 413 and 411 corresponding to $[M\text{-}107]^+$ ions, and intensities of other fragment ions were low (RA<10%), and giving limited structural information. In MS^3 (520.5→441.5→) spectrum of the GP derivatized cholestanol showed only two fragment-ions above RA of 10% at *m/z* 413 and 398 corresponding to $[M\text{-}107]^+$ and $[M\text{-}107\text{-}NH]^+$. Therefore, MS^4 ($[M]^+ \rightarrow [M\text{-}79]^+ \rightarrow [M\text{-}107]^+ \rightarrow$) spectrum were recorded. MS^4 (520.5→441.5→413.5→) spectrum shows a prominent $[M\text{-}107\text{-}CH_2NH]^+$ fragment-ion at *m/z* 384 and *m/z* 369 corresponding to the ($[M\text{-}107\text{-}NH\text{-}CH_2NH]^+$) fragment-ion, which are a partial loss of GP derivative and a typical fragmentation of steroid backbone. The MS, MS^2, MS^3 spectra for other studied authentic standards summarized in Figures S2 to S17.

3.2. Chromatographic separation of O/GP derivatized authentic standards phytosterols

Several capillary LC-MS methods were tested and summarized in Appendix A. Figure 8 shows a chromatographic separation of O/GP-derivatized authentic standards on the C_{18} column using the finalized gradient of 26-min. The O/GP derivatized 7-oxo-β-sitosterol eluted from the C_{18} column first at 6.12 min. The O/GP derivatized desmosterol eluted the second at 6.49 min. The separation of O/GP derivatized cholesterol and lathosterol was not achieved and they co-eluted at 7.38 min. However, O/GP-derivatized lathosterol gives a MS^3 spectrum a characteristic fragment-ion at *m/z* 159, which is not present in the MS^3 spectrum of cholesterol (Figure S10c). The O/GP derivatized cholestanol eluted from the LC column at 7.39 min. Phytosterols, with 9 carbons sidechain at C17 (brassicasterol and campesterol) eluted from the reversed phase column before those having 10 carbons sidechain at C17 (fucosterol, stigmasterol and β-sitosterol), showing that double bond at sidechain decrease their retention. For example, the GP derivatized brassicasterol eluted at 7.33 min before cholesterol, whereas fucosterol eluted at 7.43 min before campesterol. The location of the double bond also influences the retention on the reversed phase of O/GP derivatized stigmasterol and fucosterol, both generate a precursor ion at *m/z* 544 and have unsaturated C17 sidechain, but the O/GP derivatized stigmasterol eluted later at 7.89 min than O/GP derivatized fucosterol. Having 29 carbons and full saturation the O/GP derivatized β-sitosterol had the longest retention on the C18 column and eluted at 8.23 min. The separation of the *syn*- and *anti*-conformers was also achieved for the O/GP-derivatized campesterol, brassicasterol and β-sitosterol (Figure 8). The calibration curves and a limit of detection (LOD) and limit of quantification (LOQ) are presented in Appendix A. The chromatographic separation was also achieved for the O/GP-tagged 24S-hydroxycholesterol,

25-hydroxycholesterol, 27-hydroxycholesterol, 7β-hydroxycholesterol, 7α-hydroxycholesterol and 7α,25-dihydroxycholesterol and 7α,27-dihydroxycholesterol using the 26-min gradient (Figure S19).

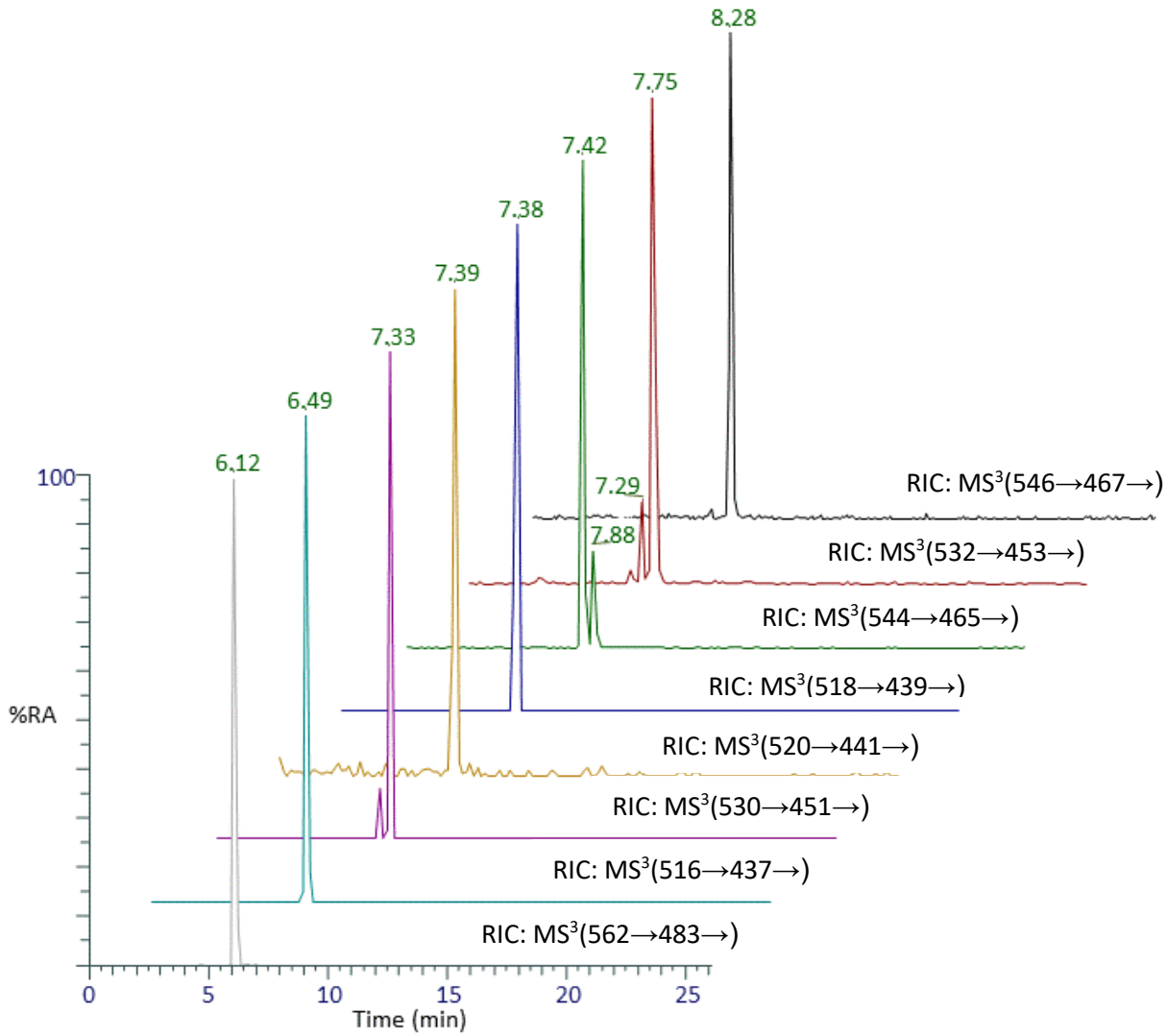

Figure 8. LC-MS Reconstructed ion chromatograms (RICs) of MS^3 transitions ($[M]^+ \rightarrow [M-79]^+ \rightarrow$) of O/GP derivatized authentic standards corresponding to:- (grey line) RT 6.12 min of the O/GP-7-oxo-β-sitosterol 562.5→483.2→, (light green) RT 6.49 min of desmosterol 516.5→437.5→, (purple) RT 7.33 min brassicasterol 530.5→451.5→, (yellow) RT 7.39 min cholestanol 520.5→441.5→, (blue) RT 7.38 min cholesterol and lathosterol 518.5→439.5→, (green) RT 7.42 min fucosterol and 7.88 min stigmasterol 544.5→465.5→, (brown) RT 7.75 min campesterol 532.5→ 453.5→, (f) RT 8.28 min β-sitosterol 546.5 467.5.

3.3. Identification of phytosterols in human serum

We adapted well validated protocol by Griffiths [46, 48] for the extraction of oxysterols but we modified this protocol to include phytosterols. Briefly, phytosterols were extracted from microliter quantities of human serum using reversed-phase (RP) solid-phase extraction (SPE) cartridge (SPE-1 protocol), we found experimentally to fully elute phytosterols require SPE-1-Fr-1 9.5 mL of 70% ethanol (an oxysterol-rich fraction), SPE-1-Fr-2 6 mL 99.9% ethanol and SPE-1-Fr-3 2 mL dichloromethane (this solvent was evaporated and this fraction was reconstituted in SPE-1-Fr-7). SPE-1 fractions were then combined as one sample (Supplemental Figure S1), followed by enzyme assisted derivatization for sterol analysis (EADSA). EADSA consists of enzymatic conversion of 3β-hydroxy-5-ene- and 3β-hydroxy-5α-hydrogen-containing sterols to 3-oxo-4-ene and 3-oxo sterols followed by derivatization with GP hydrazine to their corresponding GP hydrazones (Figure 2). To remove the excess of GP hydrazine further purification and fractionation was achieved using a recycling SPE-2 protocol using a reverse phase cartridge. As the O/GP-derivatized phytosterols are more hydrophobic than the O/GP oxysterols, cholenoic and cholestenoic acids, we determined experimentally to fully elute the O/GP derivatized cholesterol and phytosterols requires three 1-mL portions of 100% methanol (SPE-2-Fr-1, 2, 3), four 1-mL portions of 99.9% ethanol (SPE-2-Fr-4, 5, 6, 7) and two 1-mL portions of dichloromethane (SPE-2-Fr-8, 9) (Appendix A). The direct infusion MS analysis revealed the GP-tagged oxysterols and already some phytosterols were present in the first 3 mL of methanol eluent (SPE-2-Fr-1, 2, 3), whereas GP-derivatized cholesterol, phytosterols were tailed into the SPE-2-Fr-4, 5, 6, 7 and to fully elute brassicasterol, stigmasterol, desmosterol required additional SPE-2-Fr-8 (1 ml of dichloromethane). Acidic sterols eluted predominantly in the first milliliter of methanol (SPE-2-Fr-1). GP-tagged hydrazones from each SPE-2 fractions were analyzed separately and as combined aliquots of SPE-2-Fr-2, 3, 4, 5, 6, 7 fractions using the capillary LC coupled to the LTQ mass spectrometer. The identification of GP-tagged analytes was based on retention time (RTs) and MS^2, MS^3 spectra comparison with authentic standards. In the absence of authentic standards, presumptive identifications were made based on a published library of MS^3 spectra for GP-sterols.

We analyzed serum samples from patients with AHC, JSLE and healthy individuals, and identified the O/GP derivatized cholesterol, two cholesterol precursor's desmosterol and cholestanol, and five phytosterols fucosterol, campesterol, β-sitosterol, stigmasterol, brassicasterol in serum samples. An example of the O/GP derivatized fucosterol and stigmasterol identification is shown in Figure 9 from serum sample from AHC patient. RIC of

MS^3 (544.4→465.4→) transition shows chromatographic peak at RT 7.42 and MS^3 spectrum was identical to the O/GP-derivatized authentic standard fucosterol (Figure 5a), whereas an analyte eluted at RT 7.88 min was identified as the O/GP stigmasterol as its MS^3 spectrum was identical to the MS^3 spectrum of the authentic standard of O/GP-tagged stigmasterol (Figure 5b). A ratio of fucosterol-to-stigmasterol in a healthy individual was around 1.25. Figure 10a shows RIC for MS^3 (544.4→465.4→) transition, the chromatographic peaks at RT 7.42 and 7.98 min were also assigned to the O/GP-tagged fucosterol and stigmasterol in the sample from AHC patient, the ratio of fucosterol-to-stigmasterol was 10. Cholesterol and cholestanol were identified in all samples. Two adults with AHC disorder showed an increased level of campesterol and β-sitosterol in comparison to healthy individuals. AHC is a rare neurodevelopmental disorder that affects muscle movement and causes paralysis and muscle stiffness.

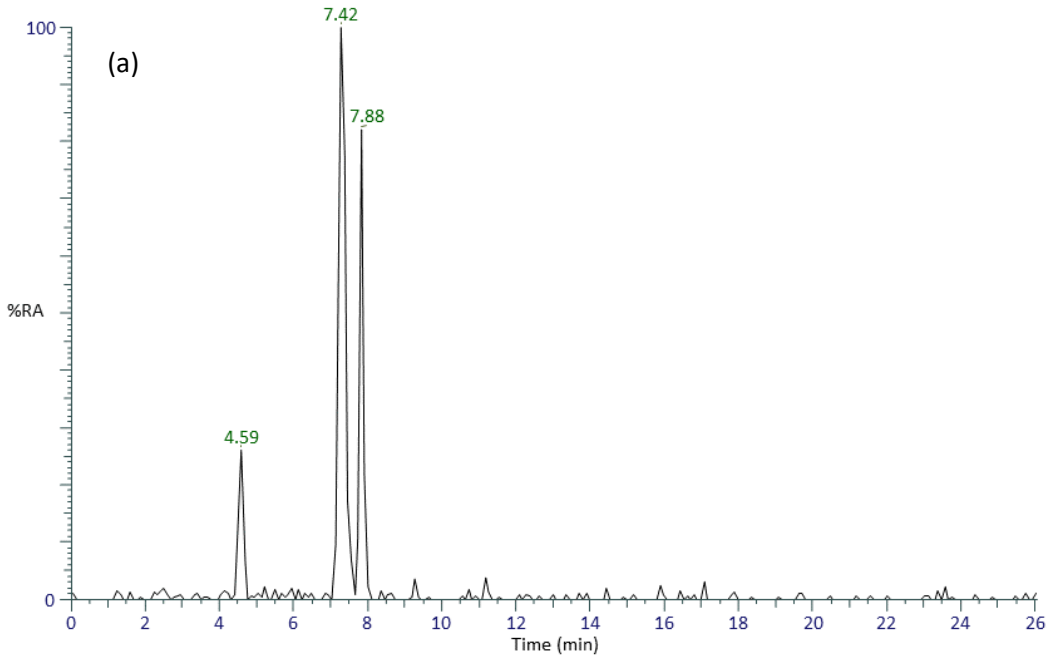

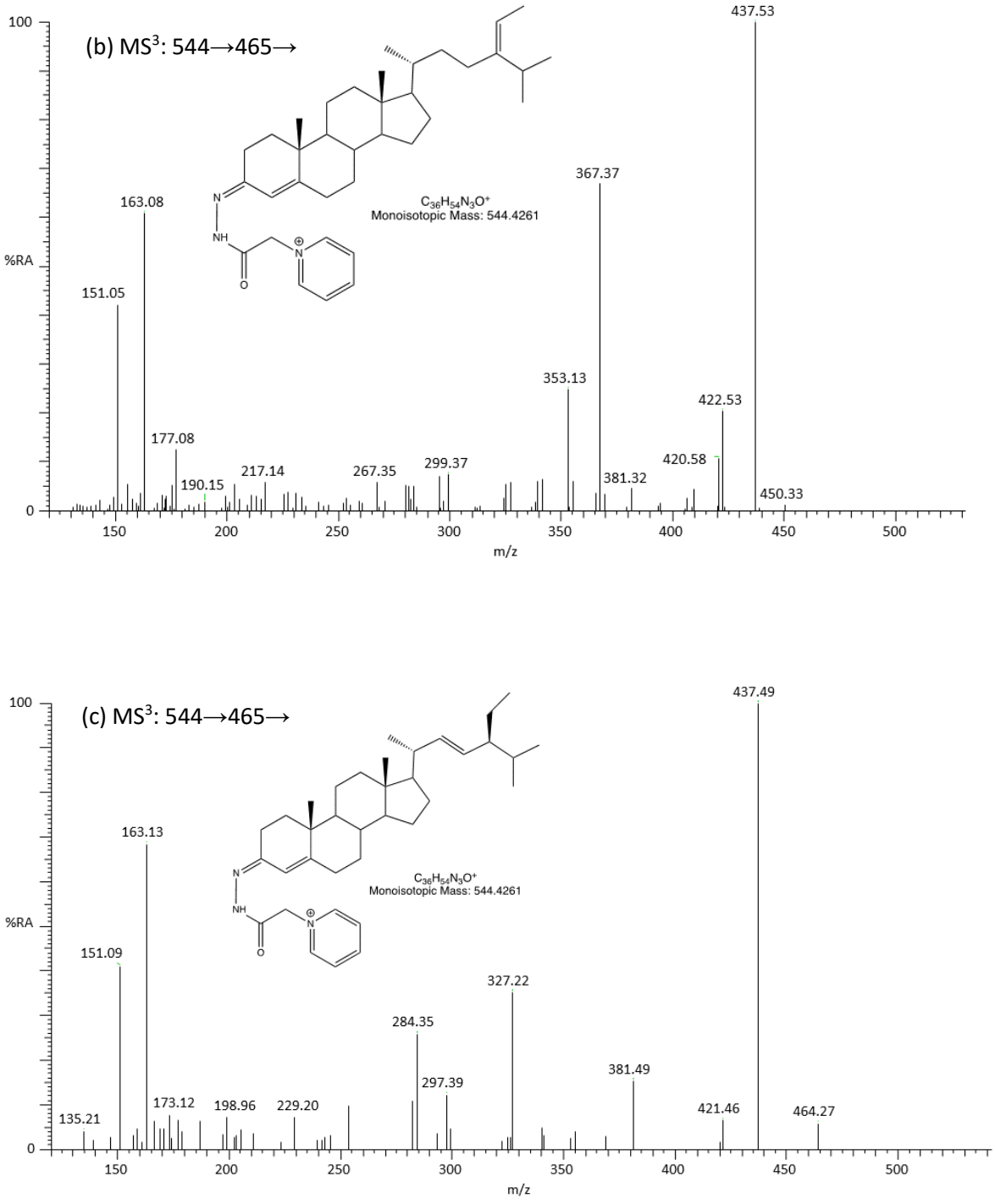

Figure 9. LC-MS^3 analysis using EADSA technology for serum sample from a healthy individual (a) RIC of MS^3 (544.4→465.4→) transition, (b) The MS^3 (544.4→465.4→) spectrum of the chromatographic peak at 7.42 min corresponding to fucosterol, (c) MS^3 (544.4→465.4→) spectrum recorded at 7.88 min corresponding to stigmasterol as identified based on comparison of RTs and MS^3 spectra with authentic standards.

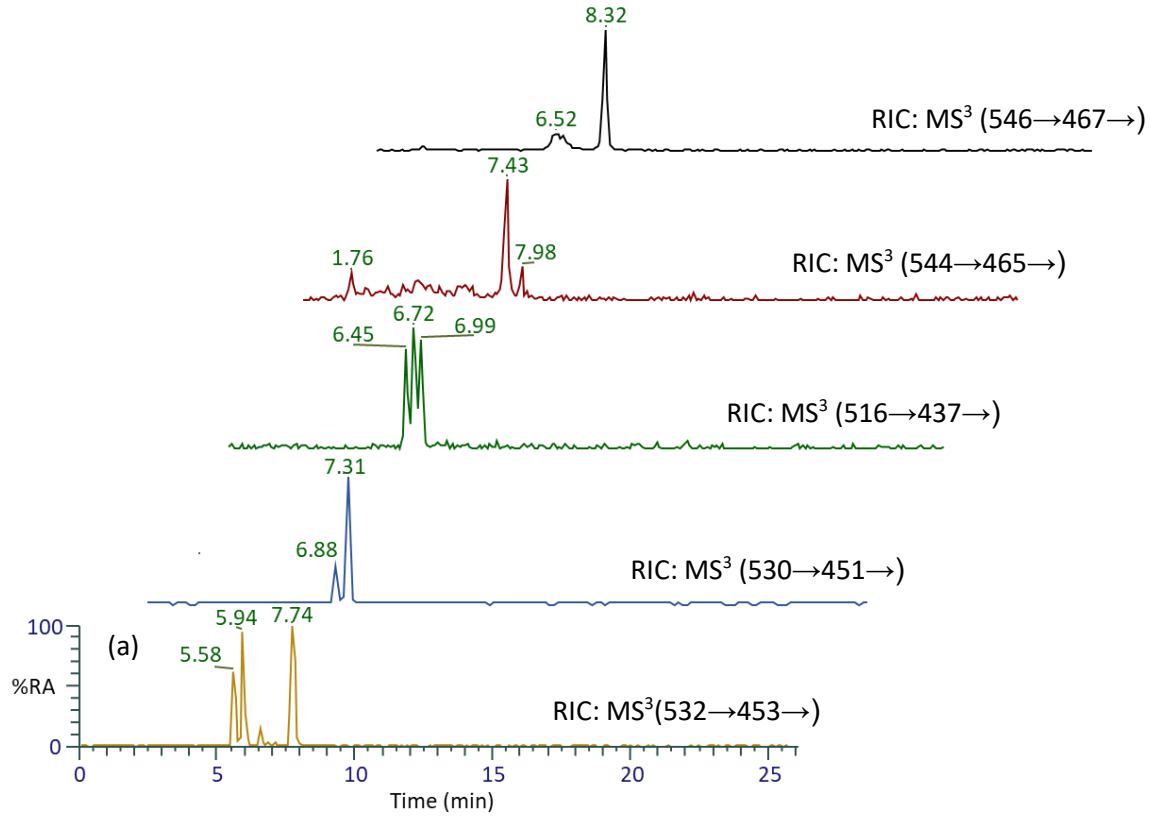

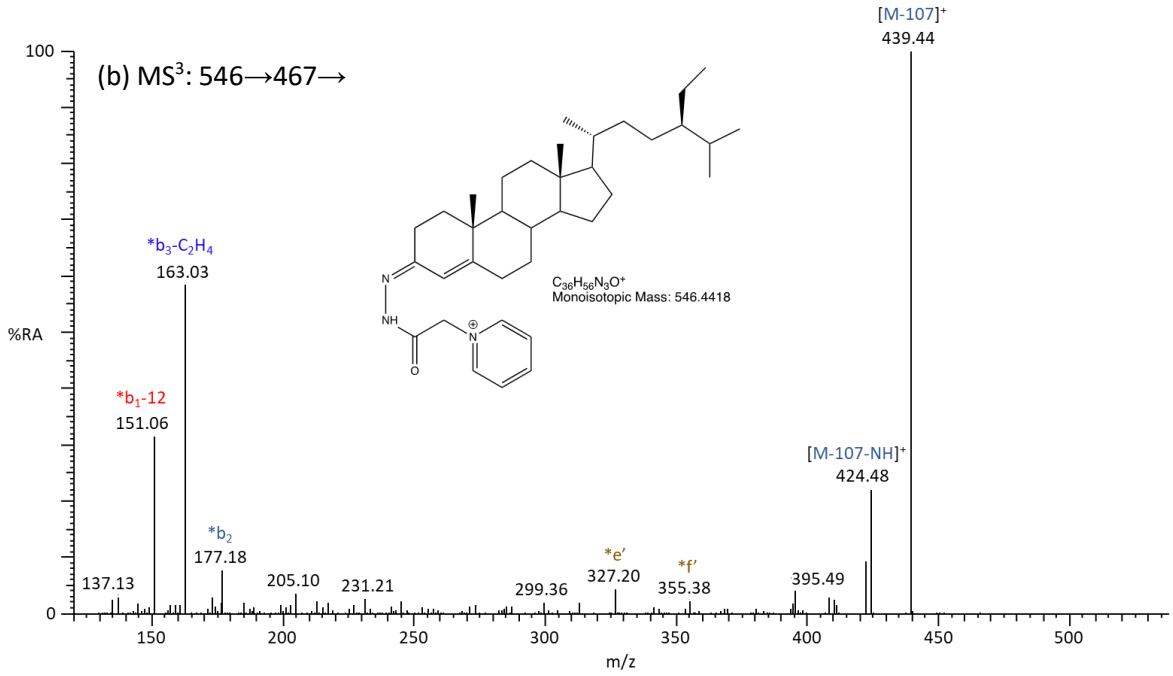

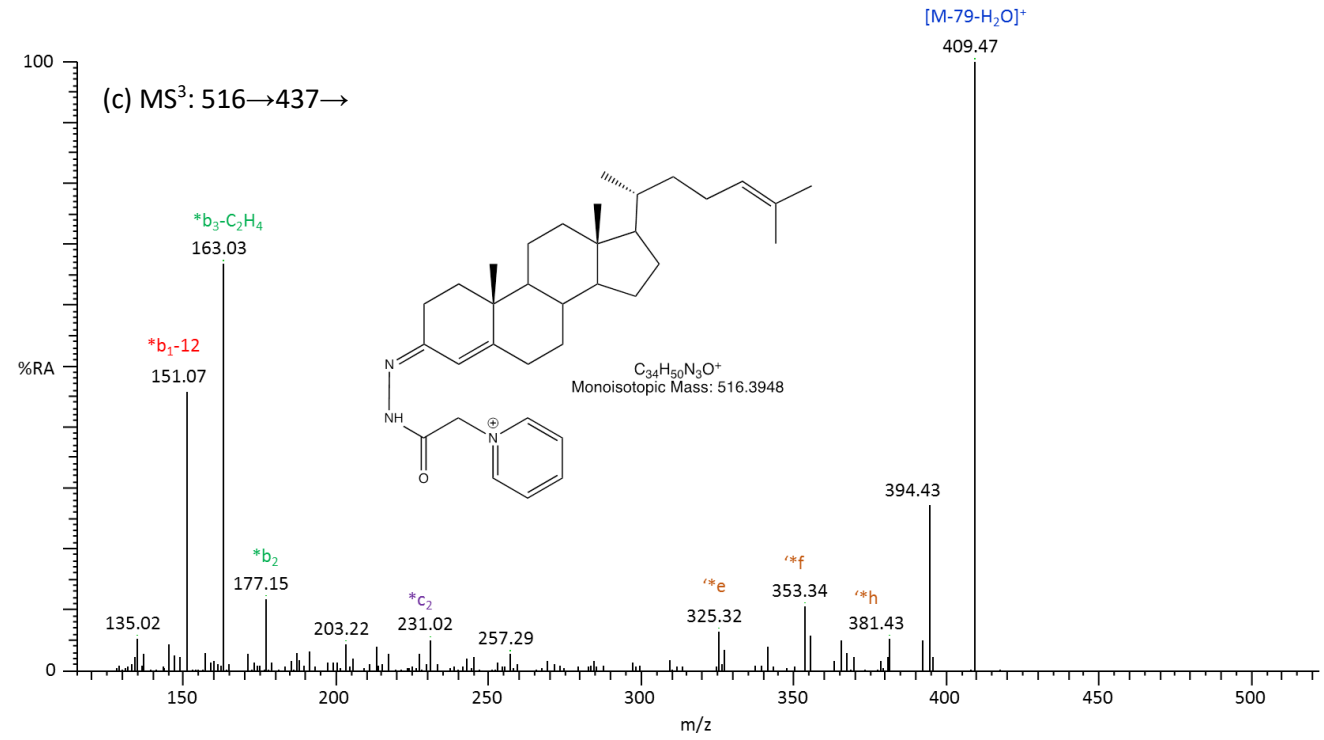

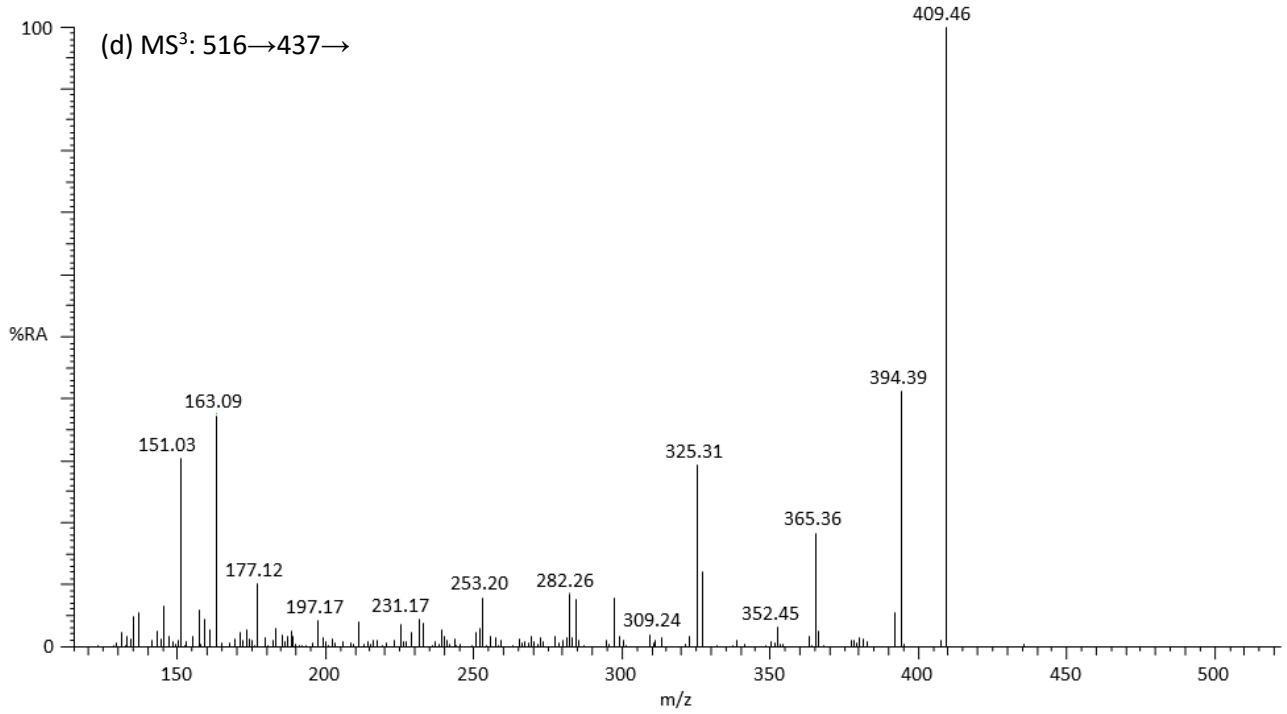

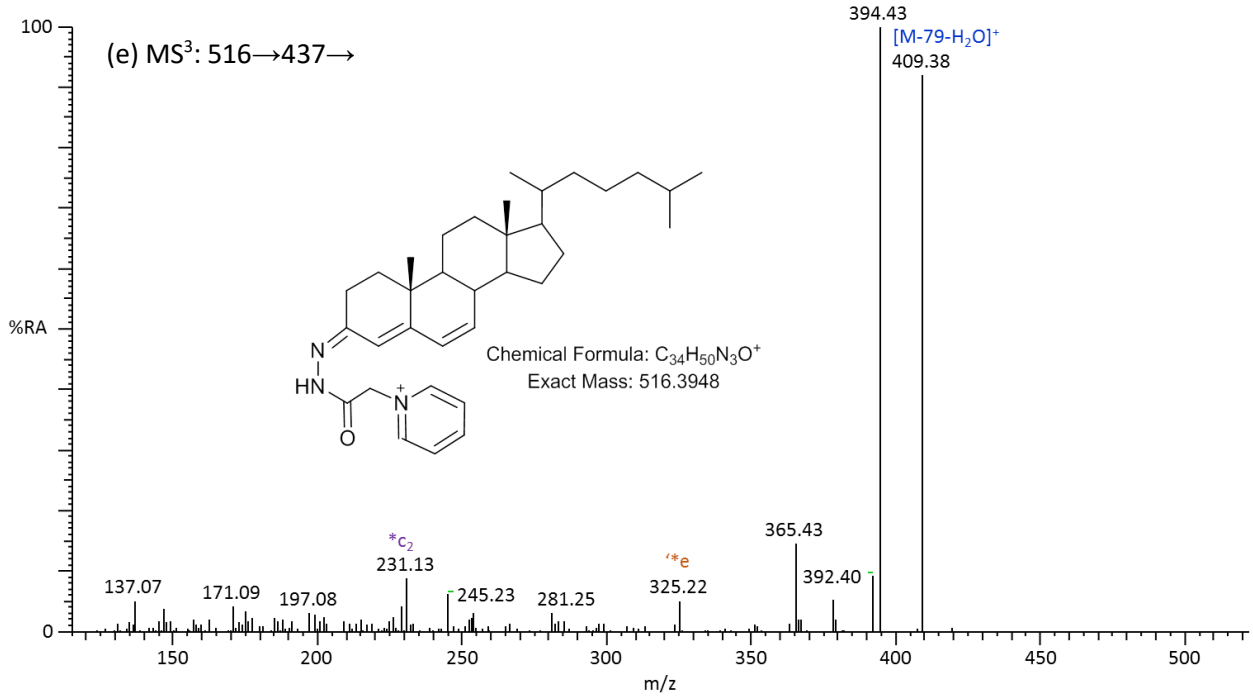

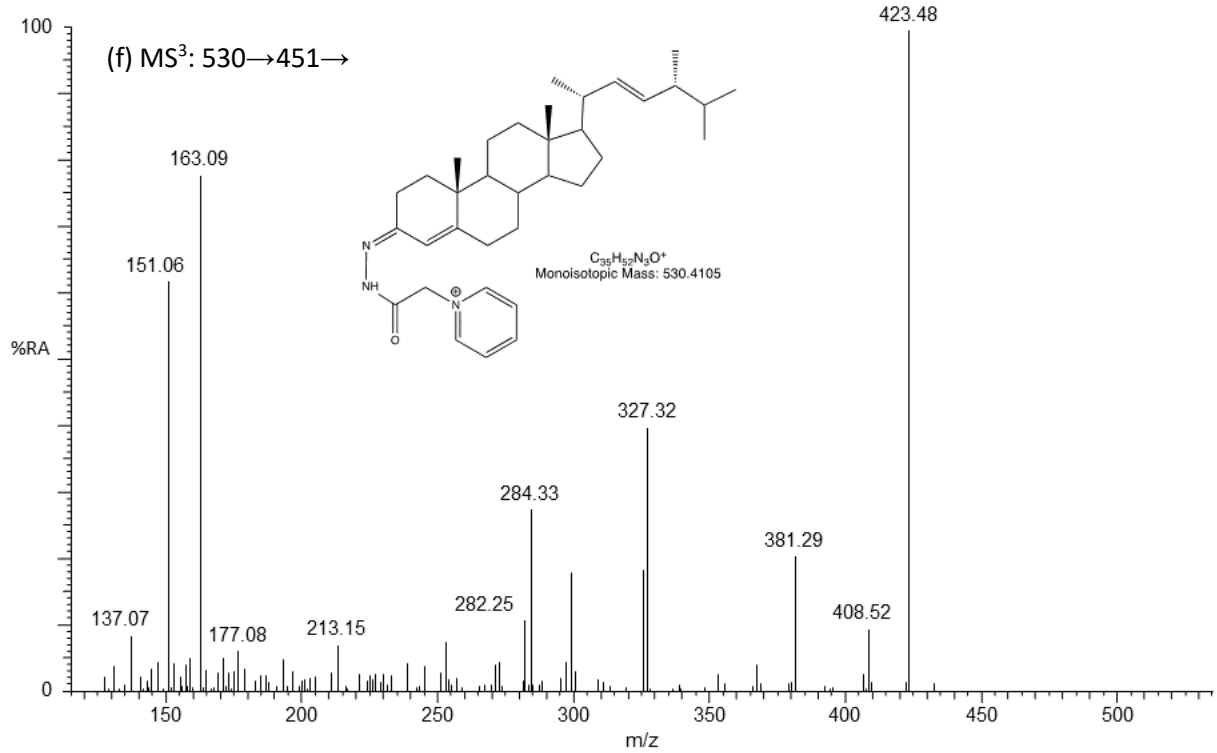

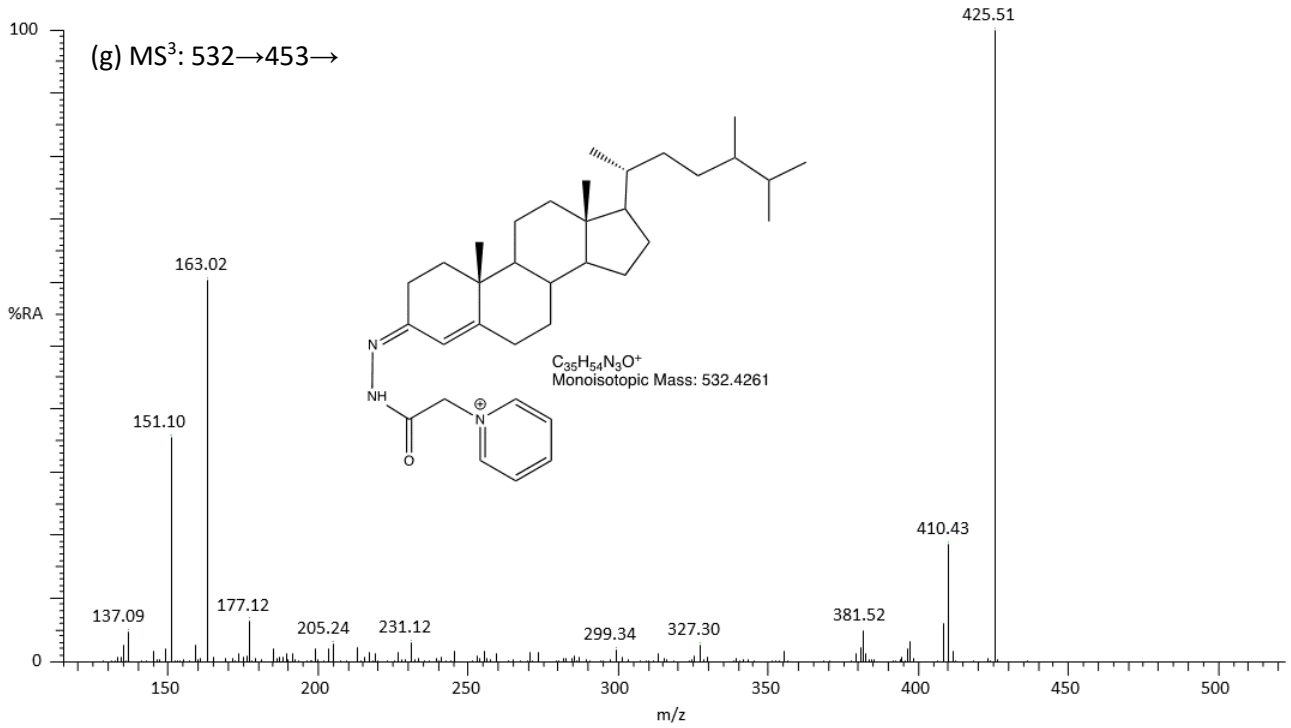

Figure 10. (a) LC-MS RICs of MS^3 ($[M]^+ \rightarrow [M-79]^+ \rightarrow$) transitions corresponding to GP-tagged physterols/sterols representative patient with AHC. The serum sample was subjected to the EADSA protocol. (b) The MS^3 (546.4→467.4→) spectrum at RT 8.32 min assigned as sitosterol, (c) MS^3 (544.4→465.4→) spectra at RT 7.43 min assigned to fucosterol and at RT 7.98 min to stigmasterol, MS^3 (516.4→437.4→) shows three components eluted at (d) RT 6.45 min peak assigned as desmoterol and at RT 6.72 min possibly cholesta-5,x-dien-3β-ol (with double bond on the side chain) and 7/8-dehydrocholesterol was assigned to the chromatographic peak at RT 6.99 min, (f) The MS^3 (530→ 451→) spectrum at RT 7.31 min was brassicasterol, (g) the chromatographic peak at RT 7.75 min for the MS^3 (532→ 453→) was identified as campesterol. The identifications were based on comparison of RTs and MS^3 spectra with authentic standards.

The following phytosterols: - campesterol, fucosterol and β-sitosterol were found in all serum samples, while stigmasterol and brassicasterol were only identified in around half of serum samples. As previously published campesterol and β-sitosterol are the most abundant phytosterols in serum [14, 51]. For example, from the RIC for the MS^3 (516.5→437.5→) transition shows three chromatographic peaks at RT 6.49, 6.73 and 7.09 min, which were in all serum samples (Figure 10a). From the MS^3 spectra of the first two chromatographic peaks at RT 6.45 and 6.72 min, the presence of *b-series indicated there was no oxygen functionality on the B-ring of steroid skeleton (Figure 10c) and RT of 6.49 min and MS^3 spectrum were identical to the O/GP-derivatized authentic standard of desmosterol. The chromatographic peak at 6.72 min did not match any literature libraries but this GP-derivatized sterol possibly corresponds to

the O/GP-derivatized cholesta-5,x-dien-3β-ol with double bond located on the side chain and an authentic standard required for positive identification (Figure 10d). The analyte eluting at RT of 6.99 min was identified as a mixture of GP derivatized 7- and 8-dehydrocholesterol by comparison with the authentic standard MS^3 spectrum (Figure 10e). Desmosterol and 7/8-dehydrocholesterol were identified in all samples.

The chromatographic peaks for MS^3 532→453→ transition at RT 5.58 min and 5.94 min (Figure 10a) were assigned to the O/GP-derivatized cholest-4-ene-3,6-dione as GP-derivatized at C-3 and C-6 positions of the steroid ring (Figure S23) and at RT 7.74 min as campesterol based on their MS^3 spectra (Figure 10a). For unknown GP-derivatized sterols for which we did not have authentic standards, we categorized them into two groups: - (a) with or (b) without *b- series fragmentation ions in their MS^3 spectra. The presence of *b- series was suspected to be sterols having no oxygen functionality on A or B ring [45]. The chromatographic peak at RT 6.84 min for RIC of MS^3 (530.4→467.4→) transition, Figure 10a, corresponds to 3β-hydroxycholesta-5,7-dien-26-oic acid as identified by comparing with MS^3 from literature [48]. The absence of *b-series fragments in MS^3 spectra were more likely to be sterols which have oxidation functionality on A or B ring, therefore the B-ring cleavage is less prominent. Figure 10a shows RIC for the transition of MS^3 (546.4→467.4→) shows the chromatographic peak at RT 6.84 min corresponds to 3β-hydroxycholesta-5,7-dien-26-oic acid as identified by comparing with MS^3 spectrum [48] and at RT 8.32 min, MS^3 of which was identical to the O/GP-tagged authentic standard of brassicasterol (Figure 10b).

Several specific MS^3 $[M]^+$→$[M-79]^+$→ transitions were set up on the linear ion trap to search for 7-hydroxy and 7-oxo- containing phytosterols such as 7-oxo-campesterol and 7-hydroxy-campesterol ($[M]^+$, *m/z* 548), sitosterol ($[M]^+$, *m/z* 562), brassicasterol ($[M]^+$, *m/z* 546), stigmasterol ($[M]^+$, *m/z* 560), fucosterol ($[M]^+$, *m/z* 560). 7-Oxo-phytosterols are a α,β-unsaturated ketone (5-en-7-one) and react with GP hydrazine in the absence of cholesterol oxidase enzyme. MS^3 ($[M]^+$→ $[M-79]^+$ →) fragmentation patterns for the 7-oxo derivatives differ from compounds with GP derivatization at carbon position C-3 as shown for the 7-oxo-β-sitosterol (Figure 6). The GP-derivatized 7-oxo-β-sitosterol was only measured in serum sample from a patient with AHC, the identification was based by RT and MS^3 spectrum of authentic standard. Figure 11 shows the RIC for 548→469→ transition, the chromatographic peak at 3.31 min corresponds to 3β-hydroxycholest-(25R)-5-en-26-oic acid. The chromatographic peak at 7.27 min possibly 3β,5α,6α-trihydroxy-sterol, as MS^3 spectrum shows a characteristic *b_2-ion at *m/z* 177 indication that sterol with a 3β-hydroxy group and a planar A/B ring system and an

unusually prominent fragment-ion observed in the MS^3 spectrum is at *m/z* 383 corresponding to $[M\text{-}H_2O\text{-}79\text{-}72]^+$ (Figure S24A). The identity of analyte eluting from the C_{18} column at RT 6.48, 6.83 and 8.83 min were not possible due to the absence of authentic standards (Figure S24B,C). There were also several oxysterols, cholestenoic acid and unknown sterols measured in samples. The identification of some characterized and non-characterized sterols which followed a typical GP derivatized sterol fragmentation pattern ($[M]^+ \rightarrow [M\text{-}79]^+ \rightarrow$) are summarized in Table S5. For those sterols not in our current library as an authentic standard, they were identified by MS^3 ($[M]^+ \rightarrow [M\text{-}79]^+ \rightarrow$) spectra comparison with published manuscripts using the EASDA technology combined with LC-MS^n analysis [25, 43, 46, 49]. Most abundant sterols were also found in all samples and their RTs and MS^3 spectra matched to cholest-4-ene-3,6-dione [45] (Figure S23), 3β-hydroxy-5-cholestenoic acid [52], 7α-hydroxy-3-oxo-4-cholestenoic acid [53], and 7α-hydroxy-3-oxochol-4-enoic acid [53] (Figure 12a,b).

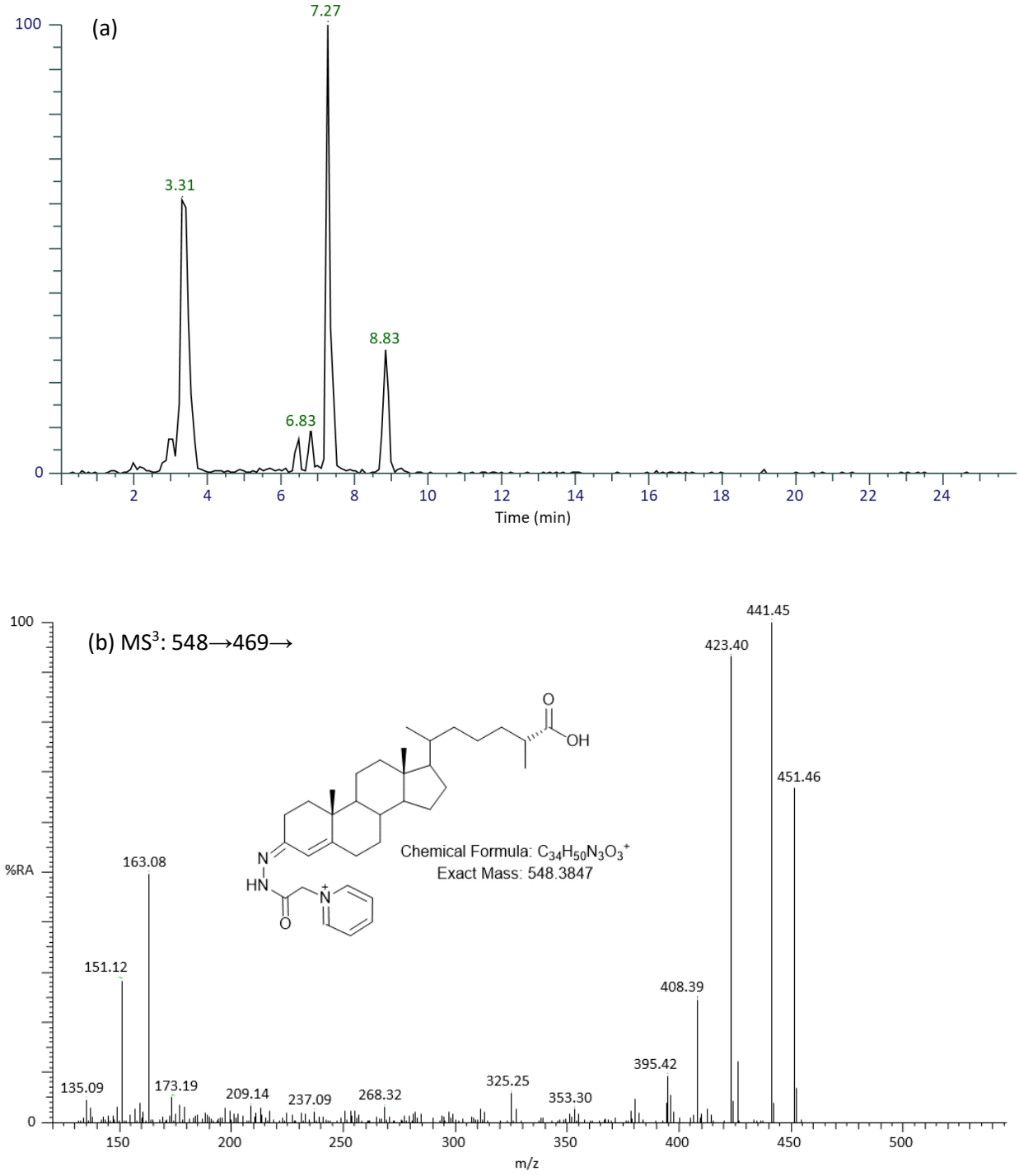

Figure 11. (a) LC-MS RICs of MS^3 (548→469→) transition corresponding to O/GP-sterols formed after EADSA protocol application using serum sample from an AHC patient. The MS^3 (548→469→) spectrum of component eluting at (b) 3.31 min corresponding to 3β-hydroxycholest-(25R)-5-en-26-oic acid.

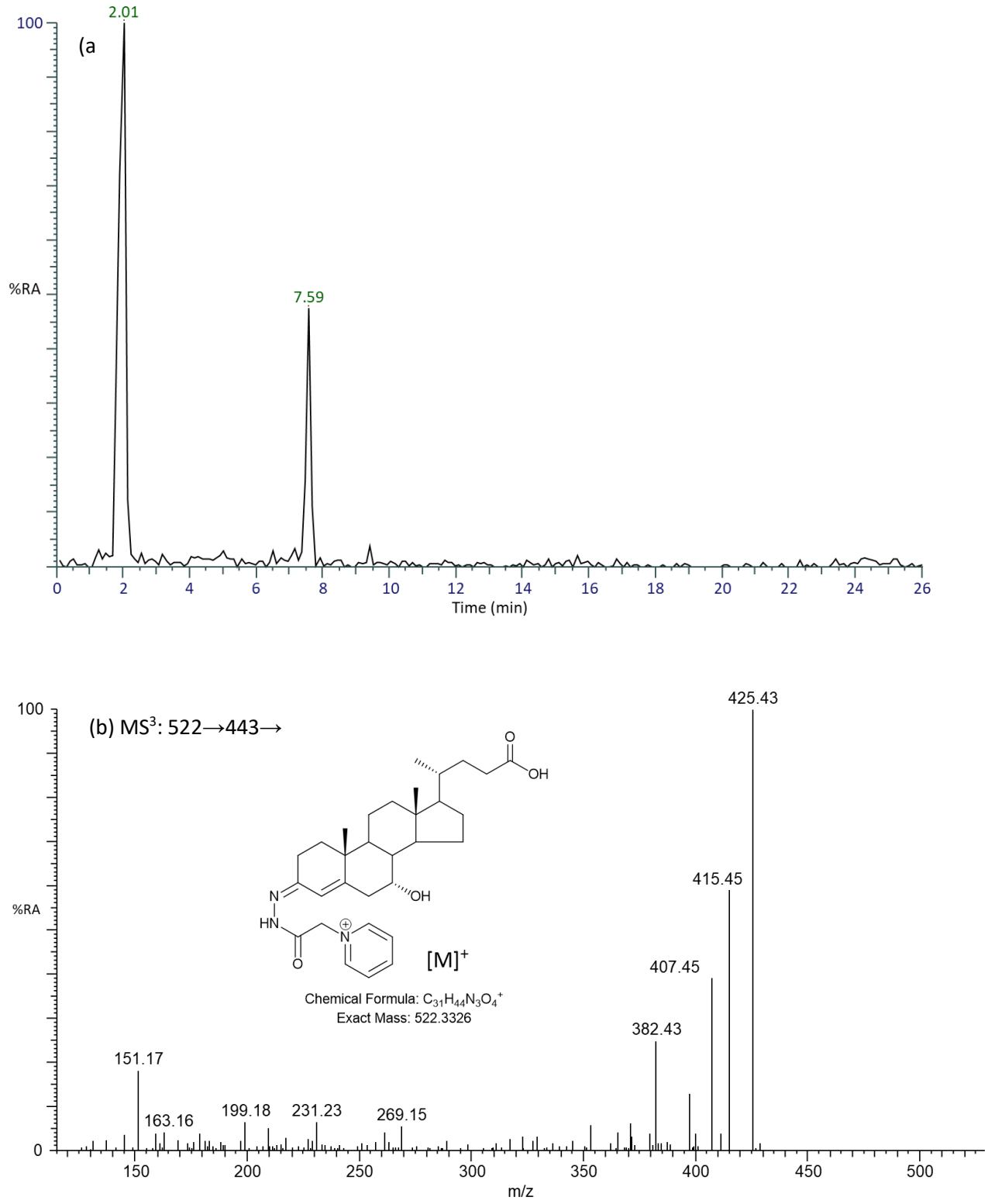

Figure 12. (a) LC-MS RICs of MS^3 (522→443→) transition, (b) MS^3 spectrum recorded at 2.01 min corresponding to the O/GP derivatized 7α-hydroxy-3-oxocholest-4-enoic acid.

The chromatographic peaks at 1.37 and 1.75 min for the transition of MS^3 (564.5→ 485.5→) correspond to 7α-hydroxy-3-oxo-4-cholestenoic acid and 3β,7α-dihydroxycholest-(25R)-5-en-26-oic acid (Figure S25A and B) as they matched to MS^3 from literature [23, 43, 49].

We analyzed samples from patients with the autoimmune rheumatic disease juvenile-onset systemic lupus erythematosus (JSLE). Juvenile-onset SLE (JSLE) is a severe inflammatory disease that can affect any part of the body, and JSLE patients are known to have altered lipid metabolism, resulting in increased risk of cardiovascular disease [54, 55]. In JSLE, these changes in lipid metabolism and potentially oxysterol metabolism are linked to a strong type 1 interferon (IFN) signature [56]. Notably, Ch25h, a key rate limiting enzyme in metabolism of cholesterol into oxysterols, is an IFN-induced gene and changes in lipid profiles in patients with JSLE are associated with inflammation [57]. It has also been demonstrated that the expression of receptors of GPR183, whose main ligand is the oxysterol 7α,25-dihydroxycholesterol, are altered in immune cells in adult-onset SLE. Taken together, this strongly suggests that oxysterol profiles are likely to alter in JSLE when compared to controls. We utilized a 21-min gradient to order to achieve better chromatographic separation for hydroxycholesterols and dihydroxycholesterols (Figure S26). We identified the O/GP 7α,25-dihydroxycholesterol, 7α,27-dihydroxycholesterol, 24S-, 25-and 27-hydroxycholesterols in patients with JSLE and healthy individuals. This preliminary analysis suggests that there is a potential reduction in 25-hydroxycholesterol in JSLE serum compared to healthy control serum with more limited differences in 7α,25-dihydroxycholesterol (Figure S27). However, more *n*-numbers are needed to confirm these preliminary results.

4. Conclusion

Phytosterols have been supplemented in functional food products for their cholesterol-lowering ability, as well as other beneficial effects, leading to increased dietary exposure of both phytosterols and their oxidation products [3, 13]. As a result, the physiological effects of phytosterols and oxidation products are constantly researched. Recent studies have suggested both phytosterols and oxyphytosterols can transverse the blood-brain-barrier and accumulate in the brain. In this work, the EADSA method with a subsequent LC-MS^n analysis was applied for the analysis of phytosterols in human serum. This method uses an extraction of phytosterols from serum, then sterols were oxidized with cholesterol oxidase and GP derivatized and analyzed using a LC-MS^n. A library of authentic standards consisted of their retention time established on the C18 column and their corresponding MS, MS^2 and MS^3 spectra was created and utilised for the identification of phytosterols in human serum. The LC-MS^n method was optimised for more hydrophobic sterols then cholesterol with a total LC run time of 26 min. The

linear range was 0.2 pg/mL to 30 ng/mL for campesterol, β-sitosterol and brassicasterol. The limit of quantification was 100 fg of the O/GP-tagged for brassicasterol and desmosterol as inject on the LC column. Phytosterols were semi-quantified using deuterated cholesterol as the internal standard. Campesterol was found at 12.00±2.68 ng/mL, β-sitosterol at 8.50±2.65 ng/mL and fucosterol was at lowest concentration at 1.50±0.84 ng/mL. This is in agreement with findings by Plant J campesterol concentration is generally higher in serum than β-sitosterol, and with the average serum circulating concentrations of cholesterol in 5 mmol/L , plant sterols 7-24 µmol/L and plant stanols 0.05 to 0.3 µmol/L [14]. Also, cholesterol, 7-oxo- β-sitosterol were also identified in human serum based on their retention time and MS^3 spectra. This methodology opens possibilities to investigate the role of phytosterols in human health and disease and could apply for the identification of oxyphytosterols in biological samples.

CRediT authorship contribution statement

Yu Chen Teng, Marie Claire Gielen, Nina De Gruijeter:- Data curation, Formal analysis, Investigation, Writing - Original Draft. Ciurtin Coziana:- Biological samples provision. Elizabeth C Rosser:- Biological samples provision, Writing- Review. Kersti Karu:- Conceptualisation, Methodology, Writing - Review & Editing, Visualization, Supervision, Project administration, Funding acquisition.

Acknowledgements

This work was supported by UCL Chemistry Department, MSc in Applied Analytical Chemistry programme. Kersti Karu is grateful to her PhD supervisors Professor William J. Griffiths and Professor Yuqin Wang (Swansea University Medical School, UK) for introducing/teaching her oxysterols and bile acids mass spectrometry analyses, and to collaborator at ThermoFisher Scientific in England, Mr Mark Sorenson. The authors thank Deepali Desai and Haoyti Minamiguchi for helping to generate figures and chemical structures drawing for this manuscript.

Appendix A. Supporting information.

Supplementary data associated with this article can be found in the online version at doi…

5. References

1. Valitova, J.N., A.G. Sulkarnayeva, and F.V. Minibayeva, *Plant sterols: Diversity, biosynthesis, and physiological functions.* Biochemistry-Moscow, 2016. **81**(8): p. 819-834.
2. Dierckx, T., J.F.J. Bogie, and J.J.A. Hendriks, *The Impact of Phytosterols on the Healthy and Diseased Brain.* Current Medicinal Chemistry, 2019. **26**(37): p. 6750-6765.
3. Hovenkamp, E., et al., *Biological effects of oxidized phytosterols: A review of the current knowledge.* Progress in Lipid Research, 2008. **47**(1): p. 37-49.
4. Lutjohann, D., et al., *Sterol Absorption and Sterol Balance in Phytosterolemia Evaluated by Deuterium-Labeled Sterols - Effect of Sitostanol Treatment.* Journal of Lipid Research, 1995. **36**(8): p. 1763-1773.
5. Jones, P.J.H., et al., *Progress and perspectives in plant sterol and plant stanol research.* Nutr Rev, 2018. **76**(10): p. 725-746.
6. Alberici, R.M., et al., *Rapid fingerprinting of sterols and related compounds in vegetable and animal oils and phytosterol enriched- margarines by transmission mode direct analysis in real time mass spectrometry.* Food Chemistry, 2016. **211**: p. 661-668.
7. Schaller, H., *New aspects of sterol biosynthesis in growth and development of higher plants.* Plant Physiology and Biochemistry, 2004. **42**(6): p. 465-476.
8. Schaller, H., *The role of sterols in plant growth and development.* Progress in Lipid Research, 2003. **42**(3): p. 163-175.
9. Schaeffer, A., et al., *The ratio of campesterol to sitosterol that modulates growth in Arabidopsis is controlled by STEROL METHYLTRANSFERASE 2;1.* Plant Journal, 2001. **25**(6): p. 605-615.
10. Vanmierlo, T., et al., *Plant sterols: Friend or foe in CNS disorders?* Progress in Lipid Research, 2015. **58**: p. 26-39.
11. Baila-Rueda, L., et al., *Simultaneous determination of oxysterols, phytosterols and cholesterol precursors by high performance liquid chromatography tandem mass spectrometry in human serum.* Analytical Methods, 2013. **5**(9): p. 2249-2257.
12. Moreau, R.A., et al., *Phytosterols and their derivatives: Structural diversity, distribution, metabolism, analysis, and health-promoting uses.* Progress in Lipid Research, 2018. **70**: p. 35-61.
13. Jie, F., et al., *Linking phytosterols and oxyphytosterols from food to brain health: origins, effects, and underlying mechanisms.* Critical Reviews in Food Science and Nutrition, 2022. **62**(13): p. 3613-3630.
14. Plat, J., et al., *Plant-based sterols and stanols in health & disease: "Consequences of human development in a plant-based environment?".* Progress in Lipid Research, 2019. **74**: p. 87-102.
15. Jimenez-Escrig, A., A.B. Santos-Hidalgo, and F. Saura-Calixto, *Common sources and estimated intake of plant sterols in the Spanish diet.* Journal of Agricultural and Food Chemistry, 2006. **54**(9): p. 3462-3471.
16. Valsta, L.M., et al., *Estimation of plant sterol and cholesterol intake in Finland: quality of new values and their effect on intake.* British Journal of Nutrition 2004. **92**: p. 671–678.
17. Jiménez-Escrig, A., A.B. Santos-Hidalgo, and F. Saura-Calixto, *Common sources and estimated intake of plant sterols in the Spanish diet.* Journal of agricultural and food chemistry, 2006. **54**: p. 3462-71.
18. Klingberg, S., et al., *Food sources of plant sterols in the EPIC Norfolk population.* European Journal of Clinical Nutrition, 2008. **62**: p. 695–703.
19. Ostlund, R.E., et al., *Gastrointestinal absorption and plasma kinetics of soy Delta(5)-phytosterols and phytostanols in humans.* American Journal of Physiology-Endocrinology and Metabolism, 2002. **282**(4): p. E911-E916.

20. Gylling, H. and P. Simonen, *Phytosterols, Phytostanols, and Lipoprotein Metabolism.* Nutrients, 2015. **7**(9): p. 7965-7977.
21. Ostlund, R.E., *Phytosterols and cholesterol metabolism.* Current Opinion in Lipidology, 2004. **15**(1): p. 37-41.
22. Wang, M.M. and B.Y. Lu, *How do oxyphytosterols affect human health?* Trends in Food Science & Technology, 2018. **79**: p. 148-159.
23. Karu, K., et al., *Nano-liquid chromatography-tandem mass spectrometry analysis of oxysterols in brain: monitoring of cholesterol autoxidation.* Chemistry and Physics of Lipids, 2011. **164**(6): p. 411-424.
24. Schött, H.F. and D. Lütjohann, *Validation of an isotope dilution gas chromatography-mass spectrometry method for combined analysis of oxysterols and oxyphytosterols in serum samples.* Steroids, 2015. **99**: p. 139-150.
25. Griffiths, W.J. and Y.Q. Wang, *Cholesterol metabolism: from lipidomics to immunology.* Journal of Lipid Research, 2022. **63**(2).
26. Griffiths, W.J. and Y. Wang, *Sterols, Oxysterols, and Accessible Cholesterol: Signalling for Homeostasis, in Immunity and During Development.* Front Physiol, 2021. **12**: p. 723224.
27. Wang, Y.Q., E. Yutuc, and W.J. Griffiths, *Cholesterol metabolism pathways - are the intermediates more important than the products?* Febs Journal, 2021. **288**(12): p. 3727-3745.
28. Ras, R.T., et al., *Intake of phytosterols from natural sources and risk of cardiovascular disease in the European Prospective Investigation into Cancer and Nutrition-the Netherlands (EPIC-NL) population.* European Journal of Preventive Cardiology, 2015. **22**(8): p. 1067-1075.
29. Mathers, J.C., *Plant foods for human health: research challenges.* Proceedings of the Nutrition Society, 2006. **65**(2): p. 198-203.
30. Griffiths, W.J., P.J. Crick, and Y. Wang, *Methods for oxysterol analysis: Past, present and future.* Biochemical Pharmacology, 2013. **86**(1): p. 3-14.
31. McDonald, J.G., et al., *A comprehensive method for extraction and quantitative analysis of sterols and secosteroids from human plasma.* Journal of Lipid Research, 2012. **53**(7): p. 1399-1409.
32. Griffiths, W.J. and Y. Wang, *Oxysterol research: a brief review.* Biochemical Society Transactions, 2019. **47**(2): p. 517-526.
33. Gachumi, G. and A. El-Aneed, *Mass Spectrometric Approaches for the Analysis of Phytosterols in Biological Samples.* Journal of Agricultural and Food Chemistry, 2017. **65**(47): p. 10141-10156.
34. Schött, H.-F. and D. Lütjohann, *Validation of an isotope dilution gas chromatography–mass spectrometry method for combined analysis of oxysterols and oxyphytosterols in serum samples.* Steroids, 2015. **99**: p. 139-150.
35. Mackay, D.S., et al., *Methodological considerations for the harmonization of non-cholesterol sterol bio-analysis.* Journal of Chromatography B-Analytical Technologies in the Biomedical and Life Sciences, 2014. **957**: p. 116-122.
36. Mast, N., et al., *Broad substrate specificity of human cytochrome P450 46A1 which initiates cholesterol degradation in the brain.* Biochemistry, 2003. **42**(48): p. 14284-14292.
37. Gachumi, G. and A. El-Aneed, *Mass Spectrometric Approaches for the Analysis of Phytosterols in Biological Samples.* J Agric Food Chem, 2017. **65**(47): p. 10141-10156.
38. Honda, A., et al., *Highly sensitive quantification of key regulatory oxysterols in biological samples by LC-ESI-MS/MS.* Journal of Lipid Research, 2009. **50**(2): p. 350-357.

39. Sidhu, R., et al., *A validated LC-MS/MS assay for quantification of 24(S)-hydroxycholesterol in plasma and cerebrospinal fluid.* Journal of Lipid Research, 2015. **56**(6): p. 1222-1233.
40. Yutuc, E., et al., *Deep mining of oxysterols and cholestenoic acids in human plasma and cerebrospinal fluid: Quantification using isotope dilution mass spectrometry.* Analytica Chimica Acta, 2021. **1154**: p. 338259.
41. Griffiths, W.J., et al., *New methods for analysis of oxysterols and related compounds by LC–MS.* The Journal of steroid biochemistry and molecular biology, 2016. **162**: p. 4-26.
42. Hong, H. and Y. Wang, *Derivatization with girard reagent T combined with LC− MS/MS for the sensitive detection of 5-Formyl-2 '-deoxyuridine in cellular DNA.* Analytical chemistry, 2007. **79**(1): p. 322-326.
43. Griffiths, W.J., et al., *Analysis of oxysterols by electrospray tandem mass spectrometry.* Journal of the American Society for Mass Spectrometry, 2006. **17**(3): p. 341-362.
44. Griffiths, W.J., et al., *Analytical strategies for characterization of oxysterol lipidomes: Liver X receptor ligands in plasma.* Free Radical Biology and Medicine, 2013. **59**: p. 69-84.
45. Karu, K., *The analysis of oxysterols by capillary liquid chromatography tandem mass spectrometry*. 2009.
46. Griffiths, W.J., et al., *Analytical strategies for characterization of oxysterol lipidomes: Liver X receptor ligands in plasma.* Free Radical Biology and Medicine, 2013. **59**: p. 69-84.
47. Griffiths, W.J., et al., *The Cerebrospinal Fluid Profile of Cholesterol Metabolites in Parkinson's Disease and Their Association With Disease State and Clinical Features.* Front Aging Neurosci, 2021. **13**: p. 685594.
48. Yutuc, E., et al., *Deep mining of oxysterols and cholestenoic acids in human plasma and cerebrospinal fluid: Quantification using isotope dilution mass spectrometry.* Anal Chim Acta, 2021. **1154**: p. 338259.
49. Wang, Y.Q., et al., *Targeted lipidomic analysis of oxysterols in the embryonic central nervous system.* Molecular Biosystems, 2009. **5**(5): p. 529-541.
50. Dickson, A.L., et al., *Identification of unusual oxysterols biosynthesised in human pregnancy by charge-tagging and liquid chromatography - mass spectrometry.* Front Endocrinol (Lausanne), 2022. **13**: p. 1031013.
51. Vanmierlo, T., et al., *The plant sterol brassicasterol as additional CSF biomarker in Alzheimer's disease.* Acta Psychiatr Scand, 2011. **124**(3): p. 184-92.
52. Dickson, A., et al., *HSD3B1 is an Oxysterol 3β-Hydroxysteroid Dehydrogenase in Human Placenta.* bioRxiv, 2022: p. 2022.04.01.486576.
53. Dickson, A.L., et al., *Identification of Unusual Oxysterols Biosynthesised in Human Pregnancy by Charge-Tagging and Liquid Chromatography - Mass Spectrometry.* bioRxiv, 2022: p. 2022.02.07.478301.
54. Robinson, G.A., et al., *Increased apolipoprotein-B:A1 ratio predicts cardiometabolic risk in patients with juvenile onset SLE.* Ebiomedicine, 2021. **65**.
55. Smith, E.M.D., et al., *Juvenile-onset systemic lupus erythematosus: Update on clinical presentation, pathophysiology and treatment options.* Clinical Immunology, 2019. **209**.
56. Wahadat, M.J., et al., *Type I IFN signature in childhood-onset systemic lupus erythematosus: a conspiracy of DNA- and RNA-sensing receptors?* Arthritis Research & Therapy, 2018. **20**.
57. Robinson, G.A., et al., *Metabolomics Defines Complex Patterns of Dyslipidaemia in Juvenile-SLE Patients Associated with Inflammation and Potential Cardiovascular Disease Risk.* Metabolites, 2022. **12**(1).